Duplicated antagonistic EPF peptides optimize grass stomatal initiation

Raman Jangra[1], Sabrina C. Brunetti[1], Xutong Wang[1,2], Pooja Kaushik[1], Patrick J. Gulick[1], Nora A. Foroud[3], Shucai Wang[4], and Jin Suk Lee[1*]

[1] Department of Biology, Concordia University, Montreal, Quebec, H4B 1R6, Canada.
[2] Key Laboratory of Molecular Epigenetics of MOE and Institute of Genetics & Cytology, Northeast Normal University, Changchun 130024, China.
[3] Lethbridge Research and Development Centre, Agriculture and Agri-Food Canada, Lethbridge, Alberta, T1J 4B1, Canada.
[4]Laboratory of Plant Molecular Genetics & Crop Gene Editing, School of Life Sciences, Linyi University, Linyi 276000, China.

[*] To whom the correspondence should be addressed: jinsuk.lee@concordia.ca

Key words:
EPF peptides, stomatal development, grass, Brachypodium

Summary statement

Duplicated antagonistic signaling peptides orthologous to the Arabidopsis EPF2 and STOMAGEN ligands, essential for the precise control of stomatal lineage initiation, in the grass model organism *Brachypodium distachyon* are revealed.

ABSTRACT

Peptide signaling has emerged as a key component of plant growth and development, including stomatal patterning, which is critical for plant productivity and survival. Although exciting progress has been made in understanding EPIDERMAL PATTERNING FACTOR (EPF) signaling in Arabidopsis, the mechanisms by which EPF peptides control different stomatal patterns and morphologies in grasses is poorly understood. Here, by examining expression patterns, overexpression transgenics, and cross-species complementation, the antagonistic stomatal ligands orthologous to Arabidopsis AtEPF2 and AtSTOMAGEN/AtEPFL9 peptides were identified in *Triticum aestivum* (wheat) and the grass model organism *Brachypodium distachyon*. Application of bioactive BdEPF2 peptides inhibited stomatal initiation, but not the progression or differentiation of stomatal precursors in Brachypodium. Additionally, the inhibitory roles of these EPF peptides during grass stomatal development were suppressed by the contrasting positive action of the BdSTOMAGEN peptide in a dose-dependent manner. These results not only demonstrate how conserved EPF peptides that control different stomatal patterns exist in nature but also suggest new strategies to improve crop yield through the utilization of plant-derived antagonistic peptides that optimize stomatal density on the plant epidermis.

INTRODUCTION

Intercellular signaling mediated by peptide ligands, which are encoded by gene families, plays a central role in plant growth and development, including stomatal patterning. Stomata are valves on the plant epidermis that control water and gas exchange between plants and the atmosphere. As such, understanding the mechanism by which stomata develop, a process that influences transpiration efficiency and plant biomass production, offers tremendous opportunity to enhance agronomic productivity (Hetherington and Woodward, 2003; Lawson and Blatt, 2014). In Arabidopsis, several members of the EPIDERMAL PATTERNING FACTOR (EPF) family of secreted cysteine-rich peptides act as cell-cell signals for proper stomatal

development. AtEPF1 and AtEPF2, the two most closely related peptides among the eleven EPF family members in Arabidopsis, are negative regulators of stomatal development. AtEPF1 controls stomatal spacing and differentiation, whereas AtEPF2 inhibits asymmetric cell divisions that initiate the stomatal cell lineage (Hara et al., 2007; Hara et al., 2009; Hunt and Gray, 2009). AtSTOMAGEN/AtEPFL9, on the other hand, was identified as a positive regulator of stomatal development, thereby functioning completely opposite to AtEPF1 and AtEPF2 peptide signaling (Hunt et al., 2010; Kondo et al., 2010; Sugano et al., 2010). Interestingly, two of these opposing stomatal signals, AtEPF2 and AtSTOMAGEN, were identified as endogenous agonistic and antagonistic ligands for the same receptor kinase ERECTA to fine-tune stomatal development in Arabidopsis (Lee et al., 2015). Some of the other AtEPF family members have also been identified as key signaling molecules controlling other developmental processes, such as the growth of inflorescence (Kosentka et al., 2019; Tameshige et al., 2016; Uchida et al., 2012; Uchida and Tasaka, 2013), highlighting the central importance of Arabidopsis EPF peptide signaling in plant growth and development.

Though plants of the grass family provide the majority of the world's food supply, many aspects of their development and physiology are less well understood than those of the model dicot species. Stomatal development in grasses differs in many ways from that in Arabidopsis (Cai et al., 2017; Chen et al., 2017; Hepworth et al., 2018). For example, unlike the two kidney-shaped guard cells in Arabidopsis, the dumbbell-shaped stomatal complexes in grasses are composed of four cells: a pair of guard cells flanked by a pair of subsidiary cells. Additionally, stomata in grasses are arranged linearly in specific cell files next to veins which are established at the base of young grass leaves, whereas in most dicot plants stomata are dispersed as a result of the formation of scattered stomatal precursors on the epidermis. Thus, one interesting question that arises from this comparison is how different stomatal patterns and morphologies are generated in the monocot crops, the answer of which may inform plant breeding strategies to for the improvement of water-use efficiency and crop biomass production. Based on the knowledge of genes regulating stomatal

development in the dicot Arabidopsis, recent investigations have started to address this important question by identifying their grass homologs. Interestingly, despite different grass stomatal morphologies and patterns, many of the grass homologs of Arabidopsis basic helix-loop-helix (bHLH) transcription factors involved in stomatal development have also been shown to control grass stomatal development, although their specific roles have diverged among different grass species (Liu et al., 2009; Raissig et al., 2016; Raissig et al., 2017; Wang et al., 2019; Wu et al., 2019). Recently, overexpression of the grass "AtEPF1" homolog, which is similar in sequence to Arabidopsis EPF1 and EPF2, has been shown to inhibit stomatal differentiation (Caine et al., 2019; Dunn et al., 2019; Hughes et al., 2017; Lu et al., 2019). In rice, homologs of AtSTOMAGEN promoting stomatal development have also been identified (Lu et al., 2019; Yin et al., 2017), but the existence of grass EPF peptide(s) regulating other aspects of stomatal development and the mechanisms of how each EPF peptide functions to control grass stomatal development remain unknown.

To understand the roles of secreted EPF peptides in grass stomatal development, we searched for entire sets of EPF homologs in the DNA sequence databases for all major cereal crops, as well as for the model grass species *Brachypodium distachyon*. These were characterized using a combination of bioinformatics, expression analyses and a series of functional genomic studies. We identified four grass EPF homologs of the well-known Arabidopsis stomatal EPFs, AtEPF1, AtEPF2 and AtSTOMAGEN that control grass stomatal development and patterning. Furthermore, using the bioactive Brachypodium EPF peptides, which were applied directly to plant seedlings to examine phenotypic responses, we found that these peptides are integral to the initiation of stomatal lineages in Brachypodium. This further corroborates that these peptides act as duplicated orthologs of the Arabidopsis AtEPF2 and AtSTOMAGEN peptides. Our finding emphasizes that despite plant species-specific differences in stomatal patterning, the stomatal initiation in both dicots and grasses depends on a precise balance of closely related EPF peptides with opposing functions.

RESULTS

Identification and expression patterns of the EPF signaling peptide family in grasses

Homologs of the Arabidopsis EPF family of signaling peptides were identified in cereal grasses by searching numerous publicly accessible databases of genomic and transcriptomic sequences. The phylogenetic analysis revealed that there are 11-15 genes per haploid genome that encode putative EPFs in each of the six grass species examined (Fig. 1, Fig. S1, Table S1). *Triticum aestivum*, which is an allohexaploid species, had 13 paralogous genes each present with three homeologous gene copies, with the exception of one that had only two homeologs. Thirteen of the 38 *EPF*-like genes of *Triticum aestivum* were either misannotated or not annotated in the V1 wheat genome assembly at Ensembl Plant, and these were corrected using comparisons to transcriptome databases (Table S2). Gene sequences for *Oryza sativa* and *Sorghum bicolor EPF* genes were taken from those previously reported (Takata et al., 2013). The initial sequences included partial-length sequences, which were supplemented with full-length sequences identified in GenBank (GB). Three additional Oryza *EPF* genes were identified in GB databases. Some members of the previously described EPF family members were removed from the set used in this study due to low sequence similarity to known *EPF* genes. As shown in Fig. S1B and Table S3, each *EPF* gene possesses six conserved cysteines in the predicted mature EPF (MEPF) domain at its C-terminal end, which are critical for the biological activity of secreted cysteine-rich peptides, including Arabidopsis EPFs. Among the 11 Arabidopsis EPF family members, stomatal EPF peptides AtEPF1, AtEPF2, and AtSTOMAGEN are the most well-characterized EPFs. Candidate orthologs of these stomatal *EPFs* were identified with two *EPF1/EPF2*-like genes, each with high sequence similarity to the C-terminus of AtEPF1 and AtEPF2, and two *STOMAGEN*-like genes found in each of the cereal genomes characterized.

To examine the potential role of grass EPF homologs in growth and development, we performed quantitative real-time PCR to analyze the expression patterns of each *EPF* gene in different organs and developmental stages in the two grass species, wheat (*T. aestivum*) and the model grass organism Brachypodium (Fig. 2A,B). In Brachypodium,

the expression of two *EPF1/EPF2*-like (*Bd5g12220* and *Bd5g23357*) and two *STOMAGEN*-like (*Bd2g58540* and *Bd3g40846*) genes, having high sequence similarity to Arabidopsis stomatal EPF peptides, was significantly greater in the aerial parts of the plants including the developing leaves, compared to the roots at both early and late stages of development. Wheat plants also showed similar expression patterns for stomatal EPF homologs, including two *EPF1/EPF2*-like genes (*TraesCS2A02G526100* and *TraesCS2A02G343000*) and two *STOMAGEN*-like genes (*TraesCS3A02G419900* and *TraesCS7A02G255900*), although *TraesCS7A02G255900* transcripts were detected at much lower levels than *TraesCS3A02G419900*. These expression patterns are consistent with their potential roles in controlling stomatal development. It is noteworthy that in a recent overexpression study of *Ta2G556200/TaEPF1B,* one of the three homeologous gene copies of *TraesCS2A02G526100* (hereafter referred to as *TaEPF1*) and *Ta2G343000/TaEPF2D,* one of the three homeologous gene copies of *TraesCS2A02G343000* (hereafter referred to as *TaEPF2*), resulted in decreased stomatal numbers with arrested stomatal precursors, a phenotype similar to the overexpression of Arabidopsis *AtEPF1* (Dunn et al., 2019). In line with previous findings in Arabidopsis (Uchida et al., 2012), the grass homologs of *AtEPFL4* and *AtCHALLAH/AtEPFL6* (*Bd1g74380*, *Bd4g15153*, *Bd2g53661*, *Bd2g22340*, *TraesCS1D02G299100*, *TraesCS4A02G028300,* and *TraesCS3A02G346000*), which are known to regulate inflorescence growth in Arabidopsis, are also expressed in the inflorescence stems of both Brachypodium and wheat. This suggests that they may play similar roles for inflorescence development in grasses. Together, these observations provide evidence that these secreted EPF peptides are active in grasses and may possibly have conserved functions in controlling various developmental processes in both dicots and grasses.

Overexpression of grass *EPF1/EPF2*-like genes restrict the initiation of the stomatal lineage, whereas *STOMAGEN*-like genes promote stomatal development in Arabidopsis

Among the family of 11 Arabidopsis EPF peptides, stomatal EPFs are the most well-characterized family members to date and the biological roles for some other EPF peptides remain unknown. Thus, to gain insight into the functional importance and conservation of grass EPF homologs, we conducted further analyses using a subset of grass EPFs that have high sequence similarity to the Arabidopsis stomatal EPF peptides. We first generated transgenic Arabidopsis plants overexpressing genes from two grass species, wheat and Brachypodium that are homologous to Arabidopsis EPF genes controlling stomatal development, using an oestradiol-induction system (Fig. 3, Fig. S2, Fig.S3). As previously reported, ectopic expression of either of the negative stomatal peptides in Arabidopsis, induced *AtEPF1* overexpression (*iAtEPF1*) and *iAtEPF2*, led to an epidermis devoid of stomata, which resulted in dramatically decreased stomatal density (number of stomata per mm^2, Fig. 2A,B,M), and thus seedling lethality (Hara et al., 2007; Hara et al., 2009; Hunt and Gray, 2009; Lee et al., 2012). However, consistent with their distinct functions during stomatal development in Arabidopsis, overexpression of *AtEPF1* led to an epidermis with arrested stomatal precursors, which resulted in a significantly increased non-stomatal cell density (number of non-stomatal epidermal cells per mm^2, Fig. 3A,M,N). In contrast, the *AtEPF2* overexpressors displayed an epidermis without any stomatal lineage cells (Fig. 3B,M,N) (Hara et al., 2007; Hara et al., 2009; Hunt and Gray, 2009). Due to their high sequence similarity to these two Arabidopsis EPF peptides, we speculated that each of the two *EPF1/EPF2*-like genes found in wheat and Brachypodium would behave like their corresponding peptides in Arabidopsis, AtEPF1 and AtEPF2, respectively. However, unexpectedly both of the *EPF1/EPF2*-like genes from Brachypodium, *iBd5g12220* and *iBd5g23357*, led to an epidermis completely devoid of all stomatal lineage cells in each of >30 T1 or T2 transgenic Arabidopsis lines examined for each construct (Fig. 3E,F,M,N, Fig. S2). Likewise, both induction of *iTaEPF1* and *iTaEPF2* overexpression resulted in inhibition of the entry of cells into the stomatal lineage, a phenotype identical to induced Arabidopsis

EPF2 overexpression (Fig. 3I,J,M,N, Fig. S3). These observations demonstrate that all examined grass homologs of *AtEPF1* and *AtEPF2* (*Bd5g12220, Bd5g23357, TaEPF1* and *TaEPF2*), when expressed in Arabidopsis, have Arabidopsis AtEPF2-like biological activity which restricts entry asymmetric divisions during stomatal development in Arabidopsis, rather than AtEPF1-like activity which inhibits later stages of development after the initiation of the stomatal lineage. Based on these findings, we named the two *EPF1/EPF2*-like genes (*Bd5g12220* and *Bd5g23357*) from Brachypodium as *BdEPF2-1* and *BdEPF2-2,* respectively.

Next, to determine the effects of ectopic expression of grass homologs of *AtSTOMAGEN*, the only positive EPF stomatal signal identified in *Arabidopsis*, we generated transgenic Arabidopsis plants overexpressing each of two *STOMAGEN*-like genes from both Brachypodium (*Bd2g58540* and *Bd3g40846*) and wheat (*TraesCS3A02G419900* and *TraesCS7A02G255900*) using an oestradiol-induction system (Fig. 3, Fig. S2, Fig. S3). Similar to the effects of *AtSTOMAGEN* overexpression, we found that inducing either copy of the grass homologs of *AtSTOMAGEN* from wheat or Brachypodium could effectively increase the production of stomata and clustering in Arabidopsis (Fig. 3G,H,K-M, Fig. S2, Fig. S3). These results indicate that these *STOMAGEN*-like genes (named *STOMAGEN-1* and *STOMAGEN-2*) are orthologs of the positive stomatal EPF peptide in Arabidopsis *AtSTOMAGEN* and have been duplicated in the genomes of both grass lineages.

Grass *EPF1/EPF2* homologs complement the epidermal phenotypes of Arabidopsis *epf2* mutants

We further investigated the behavior of two *EPF1/EPF2*-like genes from wheat and Brachypodium in the regulation of epidermal development through cross-species complementation studies. For this purpose, we expressed each of the grass *EPF1/EPF2* homologs in *epf1* and *epf2* mutants under the control of respective Arabidopsis promoters to drive their expression into distinct stages of the stomatal lineage where *AtEPF1* and *AtEPF2* are normally expressed in Arabidopsis. We first confirmed the Arabidopsis *EPF* promoters that were used for the cross-species rescue experiments drove GFP reporter activity in the corresponding stomatal

precursors in the epidermis: the *AtEPF1* promoter showed expression in late meristemoids, guard mother cells, and young guard cells; the *AtEPF2* promoter showed expression for meristemoid mother cells and early meristemoids (Fig. S4). To determine whether the grass EPF1/EPF2 peptides are functional orthologues of AtEPF1, the Brachypodium and wheat genes were expressed under the *AtEPF1* promoter in the *epf1* loss-of-function mutant. The *epf1* mutant exhibited the previously reported mild stomatal clustering phenotype, resulting from defects in spacing divisions (Fig. 4A,M) (Hara et al., 2007). Unlike the positive control (*AtEPF1pro::AtEPF1* in *epf1*; Fig. 4B,M), none of the genotypes expressing grass EPF1/EPF2 homologs (*AtEPF1pro::BdEPF2-1*, *AtEPF1pro::BdEPF2-2*, *AtEPF1pro::TaEPF1*, and *AtEPF1pro::TaEPF2*) were able to suppress *epf1's* paired stomata phenotype (Fig. 4A-F,M, Fig. S5), suggesting that neither the wheat nor the Brachypodium *EPF1/EPF2*-like genes can replace the function of *AtEPF1* in Arabidopsis. The *EPF1/EPF2*-like genes from wheat and Brachypodium were then screened for complementation of the epidermal phenotypes of *epf2*, where *epf2* displays excessive entry divisions resulting in significantly increased non-stomatal cell density (Fig. 4G,N) (Hara et al., 2009; Hunt and Gray, 2009). In this case, similar to *AtEPF2pro::AtEPF2* in *epf2* (Fig. 4H,N), expression of all grass *EPF1/EPF2* homologs driven by the endogenous *AtEPF2* promoter (*AtEPF2pro::BdEPF2-1*, *AtEPF2pro::BdEPF2-2, AtEPF2pro::TaEPF1*, and *AtEPF2pro::TaEPF2*) significantly rescued the epidermal phenotype of the *epf2* mutant (Fig. 4G-I,N, Fig. S6). These results are congruent with the results presented above on the overexpression of Brachypodium or wheat *EPF1/EPF2* homologs in Arabidopsis. Taken all together, these observations clearly indicate that either of the two most similar AtEPF1/AtEPF2 homologs from wheat and Brachypodium can substitute for AtEPF2, but they cannot replace the function of AtEPF1 in Arabidopsis.

Application of bioactive grass EPF peptides triggers stomatal developmental defects in both Arabidopsis and Brachypodium seedlings

Overexpression and cross-species complementation experiments indicated that there are two copies of stomatal EPF homologs in wheat and Brachypodium, each of which behaves like AtEPF2 and AtSTOMAGEN, respectively, when they are expressed in Arabidopsis. To determine how these grass EPF peptides regulate stomatal development in grasses, which have stomatal morphologies and patterns that differ from those of Arabidopsis, the epidermal phenotypic effects of Brachypodium seedlings (Bd21-3) treated with bioactive mature EPF peptides, MBdEPF2-1, MBdEPF2-2, and MBdSTOMAGEN-1, were examined. BdSTOMAGEN-2 was excluded from the analyses due to its relatively low level of expression in developing Brachypodium leaves, in the region where stomata develop, and also based on the functional redundancy with BdSTOMAGEN-1 in stomatal development when expressed in Arabidopsis (Fig. 2A, Fig. 3G,H,M, Fig. S2C,D). Our work focused on EPF peptides from the model grass organism Brachypodium because similar phenotypes were produced by stomatal EPF orthologs from wheat and Brachypodium in the experiments described above (Fig. 3, Fig. 4, Fig. S2, Fig. S3-S6) and because its small size allowed for the monitoring of the epidermal phenotypes on the first leaves of seedlings by bioassays. First, we produced C-terminal predicted mature forms of recombinant MBdEPF2-1 (91 amino acids), MBdEPF2-2 (83 amino acids), and chemically synthesized MBdSTOMAGEN-1 (45 amino acids) peptides based on the protocol we developed for Arabidopsis EPFs in a previous study (Fig. S7) (Lee et al., 2012). After protein refolding, we applied these bioactive grass EPF peptides to Arabidopsis seedlings. Application of either MBdEPF2-1 or MBdEPF2-2 peptide rendered the Arabidopsis epidermis completely devoid of any stomatal lineage cells resulting in a composition of only pavement cells, a phenotype identical to induced overexpression of *AtEPF2* (Fig. 5C,F,G) or application of recombinant AtEPF2 to Arabidopsis seedlings (Lee et al., 2015; Lee et al., 2012). In contrast, treatment of Arabidopsis seedlings with chemically synthesized MBdSTOMAGEN-1 promoted stomatal development and clustering, a phenotype similar to the induced

AtSTOMAGEN overexpression (Fig. 5D,H) or treatment of bioactive AtSTOMAGEN in Arabidopsis (Lee et al., 2015).

Next, to investigate whether the effects of these Brachypodium EPF peptides observed in Arabidopsis would produce similar effects in Brachypodium itself, the leaf epidermis of MBdEPF-treated Brachypodium seedlings was analyzed. Because the loss of stomata causes seedling lethality, we checked epidermal phenotypes on the first leaves of Brachypodium seedlings. As shown in Fig. 5I**,** the grass leaf epidermis in the wild-type (mock-treated Bd21-3) seedlings generated orderly patterned stomata in specific cell files typically located 1–2 cells away from veins (marked by arrowheads), unlike the scattered pattern of stomata in dicot Arabidopsis leaves. Application of either bioactive MBdEPF2-1 or MBdEPF2-2 peptide solution, however, resulted in the complete absence of any stomatal complexes at predictable distances from veins, while MBdSTOMAGEN-1 treatment promoted stomatal density and clustering in the stomatal cell files of the Brachypodium leaf epidermis (Fig. 5J-O, Fig. 6, Fig. S10B). To determine the origin of stomatal defects in MBdEPF-treated Brachypodium seedlings, we further examined 2 early stages of grass stomatal development, stomatal file establishment and asymmetric division, which can be found at the base of young Brachypodium leaves. As shown in Fig. S8, the epidermis of Bd21-3 seedlings treated with the MBdEPF2-1 or MBdEPF2-2 peptide showed neither smaller cells nor asymmetric divisions in the stomatal cell files at the predicted distances from the veins, while the application of MBdSTOMAGEN-1 to Bd21-3 seedlings resulted in ectopic files with smaller cells and asymmetric divisions. These results suggest that orthologs of AtEPF2 and AtSTOMAGEN may also be involved in regulating stomatal initiation in grasses where MBdEPF2 peptides act as inhibitors and BdSTOMAGENs act as promoters of stomatal development. However, unlike Arabidopsis, we also found that the application of either the MBdEPF2-1 or MBdEPF2-2 peptide failed to induce any obvious change to other nonstomatal epidermal cells such as silica cells in veins and hair cells, although the generation of stomata and stomatal precursors were completely blocked. The overexpression of AtEPF2 (or application of the bioactive EPF2 peptide) in Arabidopsis not only blocks stomata and stomatal precursor development but also leads to development of an

epidermis with only pavement cells. However, Brachypodium plants treated with recombinant MBdEPF2-1 or MBdEPF2-2 peptide develop hair cells instead of stomata in stomatal cell files (Fig. 5J,K,P), suggesting that the default cell fate of smaller cells of asymmetric divisions in entire epidermal lineages of grass is not affected by the application of these Brachypodium EPF peptides. On the other hand, Brachypodium seedlings treated with MBdSTOMAGEN-1 displayed variability in the strength of the phenotype, and the seedlings showing the strongest epidermal phenotypes exhibited some unusual subsidiary cell morphologies and additional ectopic stomatal cell files, in addition to increased stomatal density and stomatal patterning defects (Fig. S9A). Because Brachypodium leaves produce highly spatially and temporally organized stomatal development from the base to the tip, we next examined potential roles of BdSTOMAGEN-1 in later stages of grass stomatal development by observing cells at subsidiary cell formation and guard mother cell division stages. As shown in Fig. S9B, application of MBdSTOMAGEN-1 to Brachypodium seedlings displayed abnormal subsidiary cell formation either by spanning multiple smaller daughter cells, becoming stomatal precursors (guard mother cells, GMCs), or by producing extra irregular asymmetric divisions in the cells neighboring the GMCs. This indicates that BdSTOMAGEN-1 may have an additional role in promoting asymmetric divisions to produce both stomatal precursors and subsidiary cells, in addition to initiating stomatal cell files during grass stomatal development. In summary, our data indicates that Brachypodium EPF peptides BdEPF2s and BdSTOMAGENs are key secreted signaling peptides with opposing functions in controlling stomatal initiation in Brachypodium. Unlike BdEPF2s, which specifically control the early step of grass stomatal development (the establishment of stomatal cell files), our results also suggest that BdSTOMAGEN regulates several stages of stomatal development and patterning in grasses.

Duplicated grass EPF peptides, BdEPF2 and BdSTOMAGEN, compete for grass stomatal development

Given that both BdEPF2-1 and BdEPF2-2 inhibit grass stomatal initiation while BdSTOMAGENs act as stomata-inducing signals, we next examined whether biological activity of these BdEPF2 peptides is inhibited by the contrasting BdSTOMAGEN peptide. Application of either MBdEPF2-1 or MBdEPF2-2 peptide to Brachypodium wild-type seedlings inhibited stomatal development as described above, but by co-incubating with increasing concentrations of BdSTOMAGEN-1 peptide, the stomataless phenotype was restored to a nearly normal epidermis with stomata in a dose-dependent manner (Fig. 6). To ensure the specificity of these results, we also refolded chemically synthesized MBd2g53661 peptide, another member of the EPF-family in Brachypodium, which our expression analysis indicated is expressed in young leaves where stomata develop (Fig. 2A, Fig. S7). As shown in Fig. S10, exposure of both Arabidopsis and Brachypodium seedlings to MBd2g53661 peptide solution demonstrated that the Bd2g53661 peptide does not have a role in stomatal development, unlike the grass EPF peptides we have investigated. Exposure of Bd21-3 seedlings to mixtures of bioactive MBdEPF2-2 plus higher concentrations of MBd2g53661 peptide did not affect MBdEPF2's capacity to inhibit stomatal development in Brachypodium (Fig. S10B). This clearly indicates that the effects of the positive regulator MBdSTOMAGEN on two MBdEPF2-treated stomataless Brachypodium epidermises are the result of their specific antagonistic behaviors in controlling grass stomatal development. Since BdSTOMAGEN-1-treated Brachypodium seedlings often develop stomata with unusual subsidiary cell morphologies (Fig. S9), we also investigated the effect of MBdEPF2-2 on the subsidiary cell defects found on MBdSTOMAGEN-1-treated Brachypodium epidermises. The stomata-inducing phenotype of the MBdSTOMAGEN-1 application was suppressed by MBdEPF2-2, but the subsidiary cell defect phenotype of MBdSTOAGEN-1-treated seedlings was unaffected by the MBdEPF2-2 application (Fig. S11). This result further emphasizes the antagonistic relationship of BdEPF2 and BdSTOMAGEN is specific to the early stage of stomatal development in Brachypodium.

DISCUSSION

The present study aimed to identify EPF peptides and their biological functions in grasses since this group of plants includes several of the most important agricultural crops, and because grasses generally have different developmental processes than those of dicots. We discovered that all major cereal plants examined have genes encoding 11–15 putative EPF peptides, including at least two homologs of *AtEPF1* and *AtEPF2* and two *AtSTOMAGEN*-like genes, suggesting that the EPF family of secreted cysteine-rich peptides are conserved signaling molecules between dicots and grasses. Our work also revealed that four grass EPF peptides, which are homologs to known stomatal Arabidopsis EPFs, are duplicated grass orthologs of AtEPF2 and AtSTOMAGEN, and these two classes of signalling peptides have opposing activity in controlling the early stage of stomatal development, stomatal cell file establishment, in grasses.

In Arabidopsis, although two negative stomatal signals, AtEPF1 and AtEPF2, have a strong sequence similarity, these EPF peptides control two distinct steps of stomatal development: AtEPF1 inhibits stomatal differentiation and enforces spacing division, and AtEPF2 inhibits initiation of stomatal cell lineage (Hara et al., 2007; Hara et al., 2009; Hunt and Gray, 2009). Recent studies for *AtEPF1/AtEPF2*-like and *STOMAGEN*-like genes in some grass species indicate that they have a role in controlling stomatal differentiation (Caine et al., 2019; Dunn et al., 2019; Hughes et al., 2017; Lu et al., 2019; Yin et al., 2017). For example, overexpression of one of the *AtEPF1/AtEPF2*-related genes in barley, *HvEPF1*, decreased stomatal density, but like Arabidopsis *EPF1* overexpressor, it also significantly increased non-stomatal cells by increasing the density of arrested stomatal precursors (Hughes et al., 2017). By contrast, our functional analyses for two *AtEPF1/AtEPF2*-like genes found in wheat (*TaEPF1* and *TaEPF2*) and Brachypodium (*BdEPF2-1* and *BdEPF2-2*) demonstrated that they all play an important role in regulating stomatal initiation rather than stomatal differentiation or progression, which indicates that *AtEPF1/AtEPF2*-like genes in these two species behave like Arabidopsis *EPF2* (Fig. 3, Fig. 4, Fig. S2-S6). Our conclusion concerning the function of the two grass EPF1/EPF2-like peptides examined was further supported by bioassays with the predicted mature

Brachypodium EPF (MBdEPF) peptides. Like *AtEPF2* overexpression (or application of mature AtEPF2 peptide), the application of either of the bioactive, recombinant EPF1/EPF2-like peptides from Brachypodium, MBdEPF2-1 and MBdEPF2-2, led to an epidermis completely devoid of any stomatal precursors and stomata in both Arabidopsis and Brachypodium, a result that is similar to the overexpression of Arabidopsis's *AtEPF2* overexpression, or the treatment with the mature AtEPF2 peptide (Fig. 5, Fig. 6, Fig. S8). On the other hand, another EPF peptide homolog in Brachypodium, MBd2g53661, was found to not affect stomatal development (Fig. S11). Thus, consistent with our overexpression and cross-species complementation studies, these results clearly indicate the specific roles for BdEPF2-1 and BdEPF2-2 in inhibiting entry into the stomatal lineage during stomatal development in both Arabidopsis and Brachypodium. Our findings demonstrate how various grass species use conserved EPF peptides differently in order to control stomatal development, which highlights the importance of examining multiple species in order to fully understand the function of each EPF family member in grass stomatal development.

The difference in observations for the effects of TaEPF1 and TaEPF2 reported here, and those reported in barley (*Hordeum vulgare*) for HvEPF1 (Hughes et al., 2017), are somewhat surprising since *T. aestivum m* and *H. vulgare* are phylogenetically very closely related, and the active peptides for the two species differ by only 2 amino acids out of 52; in contrast, TaEFP1 and TaEPF2 are only 78% similar. While this paper was in preparation, Dunn et al. (2019) reported that overexpression of *EPF1/EPF2*-like genes from *T. aestivum* led to slight stomatal reduction with increased non-stomatal cell density. There are subtle differences in the experimental methods in these studies that may contribute to these differences. Since the loss of stomata is typically lethal, we used a chemically inducible gene expression technique that allowed quantitative induction of transgene expression, allowing some circumnavigation around the lethal effects of overexpressing key stomatal regulators. Both the two EPF1/EPF2-like peptides from Brachypodium, and those from wheat, inhibited stomatal development in transgenic Arabidopsis as effectively as the native Arabidopsis EPF2, which was also clearly observed with the treatment of plants with recombinant MBdEPF2 peptides (Fig. 3, Fig. 6). Hughes et al (2017) and Dunn et al

(2019), on the other hand, used transgenic plants with constitutive overexpression, and they reported that overexpression of *HvEPF1* (and *TaEPF1* or *TaEPF2*) was not able to reduce stomatal density as much as that of Arabidpsis EPF1 or EPF2. It is possible that the different phenotypes observed did not include the strongest phenotypic classes, those completely lacking stomata produced by overexpression of *HvEPF1,* since such plants may not have survived, and the plants that were characterized had low to moderate levels of transgene expression (Dunn et al., 2019; Hughes et al., 2017). Other subtle differences in experimental methods, such as dosage and timing of the treatment, may also contribute to these differences, and future studies of the spatial and temporal expression of EPF peptides in each grass species may help our understanding of how each grass EPF controls stomatal patterning and the major stages of grass stomatal development. As mentioned above, the application of recombinant MBdEPF2 peptides to Brachypodium inhibited the development of stomata within stomatal cell files but did not influence any other epidermal cell types, such as hair cells. This specific behavior found in Brachypodium seedlings might be attributed to grass-specific stomatal development patterns, which have evolved different roles for EPF1 and EPF2 in Arabidopsis that are not observed for grasses, exemplified here by wheat and Brachypodium.

The functions of other grass EPF gene family members, other than those of the four EPF homologs of Arabidopsis stomatal peptides AtEPF1, AtEPF2, and AtSTOMAGEN that we have investigated, remain completely unknown. Considering that some grass EPF family members, such as *Bd3g58660* and *Ta2g317000*, are highly expressed in young leaves where stomata develop in Brachypodium and wheat (Fig. 2A,B), it is possible that other grass EPF family members, which we identified by phylogenetic analyses, serve as ligands to control different stages of grass stomatal development such as asymmetric division to create stomatal precursors or their grass-specific adjacent subsidiary cells and stomatal differentiation. Thus, future investigation of the remaining grass EPF homologs would provide comprehensive insight into the role of EPF peptide signaling in grass developmental processes, including stomatal patterning.

Though the EPF1, EPF2 and STOMAGEN peptides have been shown to interact with TMM and ERECTA-family receptor kinases, none of the work with grass homologs of Arabidopsis stomatal receptors have yet demonstrated the roles of orthologous receptors in grass stomatal development. The existence of antagonist regulation of grass stomatal development by duplicated orthologs of Arabidopsis AtEPF2 and AtSTOMAGEN suggests that stomatal initiation in both plant species may be regulated by naturally occurring agonistic and antagonistic ligands for the same receptor, despite differences in their stomatal patterns. Application of either the MBdEPF2-1 or MBdEPF2-2 peptide to Brachypodium wild-type seedlings inhibited stomatal development, while its co-incubation with increasing concentrations of MBdSTOMAGEN-1 resulted in a nearly normal stomatal density without increased stomatal clustering even when Brachypodium seedlings were treated with very high concentrations of MBdSTOMAGEN-1 compared to the MBdEPF2 peptide (Fig. 6, Fig. S9). Thus, unlike Arabidopsis, where AtSTOMAGEN and AtEPF2 peptides directly compete for the ERECTA receptor kinase, it is possible that positive and negative stomatal EPF peptides in grasses have different target receptors, thereby influencing each other's signaling indirectly, or they may bind to the same receptor but with a different binding affinity.

Besides regulating the entry into the stomatal lineage, we found that BdSTOMAGENs may regulate many aspects of stomatal development (i.e., subsidiary cell formation) in Brachypodium. In rice, the loss of one of *STOMAGEN*-like gene, *OsEPFL9-1*, resulted in reduced stomatal formation, however overexpression of another rice *STOMAGEN*-like gene, *OsEPFL9-2,* in Arabidopsis showed mild hypocotyl-specific stomatal patterning defects, suggesting their divergent roles in rice stomatal development (Lu et al., 2019; Yin et al., 2017). These differences indicate that although different grass species use homologs of well-known stomatal AtEPFs, they may regulate their stomatal development in a species-specific manner. Future investigation on the linkage of grass STOMAGENs to distinct stages of grass stomatal development or to a specific organ, presumably by expressing BdSTOMAGEN under the control of each organ-specific or grass stomatal lineage cell type-promoters, will provide insight to how BdSTOMAGENs function in a specific

phase, or organ, of grass stomatal development. The work presented herein shows that the regulation of stomatal development by secreted EPF peptides is, to a great extent, conserved in two major classes of flowering plants, and it creates significant potential for the agricultural use of peptide treatments to improve crop productivity and water-use efficiency.

MATERIALS AND METHODS

Plant materials and growth conditions

The Arabidopsis ecotype Columbia (Col) was used as a wild-type control in the Arabidopsis study. The following mutants and transgenic plants were described previously: *epf1* (Hara et al., 2007), *epf2* (Hara et al., 2009), *proEst::AtEPF1* and *proEst::AtEPF2* (Lee et al., 2012)*, and proEst::AtSTOMAGEN* (Lee et al., 2015). Each transgene was introduced into Col and respective mutant backgrounds by *Agrobacterium*-mediated transformation. The wheat (*Triticum aestivum L.)* genotype Chinese Spring was used for isolation of gene sequences and expression analysis. Brachypodium line Bd21-3 was used for isolation of gene sequences, expression studies, and peptide bioassays. Seeds were surface sterilized with bleach solution (with 3.4% sodium hypochlorite (diluted from 10.3 % bleach), 0.01 % Triton-X 100) and plated on ½ Murashige-Skoog (MS) agar plates. When needed, 5- to 6-day-old Brachypodium and wheat seedlings and 10-day-old Arabidopsis seedlings were transferred to soil and grown at 22°C under the long-day conditions (18h light/6h dark).

Phylogenetic analysis

The amino acid sequences of the known or predicted mature EPF peptides previously identified in Arabidopsis and rice (Takata et al., 2013) were used as query sequences to identify homologous gene sequences for *Triticum aestivum* in the Transcriptome Shotgun Assembly (TSA) databases of the National Center for Biological Information (NCBI) by tBlastn. The TSA contigs were used to search the NCBI EST database and the International Wheat Genome Sequencing Consortium

(IWGSC) (International Wheat Genome Sequencing, 2014) of wheat survey sequences (WSS) of individual chromosome arms, versions 2 and 3. The sequences were also re-confirmed, and assigned to specific wheat chromosomes using the IWGSC whole genome assembly RefSeq v1.0 (Alaux et al., 2018; International Wheat Genome Sequencing, 2014; International Wheat Genome Sequencing et al., 2018). Comparison to the sequences of the whole genome assembly was used to identify homeologous copies of the gene family members from the A, B and D genomes of *T. aestivum*. Novel sequences identified in genomic databases were iteratively used to query the TSA and EST databases to verify the sequences and to correctly identify the exon/intron junctions in the genomic sequences. In cases where there was discrepancy between sequences from different databases, contigs of the transcripts were re-assembled with *T. aestivum* EST sequences that shared a minimum of 99% identity using the CAP3 assembly program at PRABI (Huang and Madan, 1999). Gene identifiers for *T. aestivum* used in the manuscript are from the Ensembl Plant database (http://plants.ensembl.org/) and those for Brachypodium are from the Phytozome 12 database (https://phytozome.jgi.doe.gov/). *EPF* gene family members identified in *T. aestivum* were used to identify homologs in other monocotyledonous species. Sequences for *EPF* genes in other species were taken from the following databases: *Sorghum bicolor,* PlantGDB (http://www.plantgdb.org/SbGDB/); *Oryza sativa,* Rice annotation project database (https://rapdb.dna.affrc.go.jp/); *Zea mays,* GenBank, (https://www.ncbi.nlm.nih.gov/); *Brachypodium distachyon,* Phytozome v12 (https://phytozome.jgi.doe.gov/); *Hordeum vulgare,* IPK (http://webblast.ipk-gatersleben.de/); *Arabidopsis thaliana,* UniProt (https://www.uniprot.org/uniprot/). An initial phylogenetic tree for the heuristic search was obtained automatically by applying Neighbor-Joining and BioNJ algorithms to a matrix of pairwise distances estimated using a Jones Taylor Thornton (JTT) model and then selecting the topology with superior log likelihood value. The analysis involved 87 amino acid sequences. All positions with less than 95% site coverage were eliminated. That is, fewer than 5% alignment gaps, missing data, and ambiguous bases were allowed at any position. These procedures were performed

using MEGA software (version 7.0) (Kumar et al., 2016). See Table S1 and Table S2 for details on the list of amino acid sequences of grass EPF peptides used.

Plasmid construction and generation of transgenic plants

The following constructs were generated and used in this study: pJSL156 (*BdEPF2-1* cDNA), pJSL151 (*proEst::BdEPF2-1*), pJSL157 (*BdEPF2-1* cDNA), pJSL158 (*proEst::BdEPF2-2*), pJSL148 (*BdSTOMAGEN-1* cDNA), pJSL149 (*proEst::BdSTOMAGEN-1*), pJSL185 (*BdSTOMAGEN-2* cDNA), pJSL187 (*proEst::BdSTOMAGEN-2*), pJSL171 (*TaEPF1* cDNA), pJSL179 (*proEst::TaEPF1*), pJSL173 (*TaEPF2* cDNA), pJSL180 (*proEst::TaEPF2*), pJSL177 (*TaSTOMAGEN-1* cDNA), pJSL181 (*proEst::TaSTOMAGEN-1*), pJSL188 (*proEst::TaSTOMAGEN-2*), pJSL193 (*AtEPF1* cDNA), pRJ14 (*proAtEPF1::nucGFP*), pRJ21 (*proAtEPF1::AtEPF1*), pRJ6 (*proAtEPF1::BdEPF2-1*), pRJ13 (*proAtEPF1::BdEPF2-2*), pRJ9 (*proAtEPF1::TaEPF1*), pRJ18 (*proAtEPF1::TaEPF2*), pJSL146 (*AtEPF2* promoter), pJSL194 (*AtEPF2* cDNA), pRJ23 (*proAtEPF2::nucGFP*), pRJ22 (*proAtEPF2::AtEPF2*), pJSL175 and pRJ17 (*proAtEPF2::BdEPF2-1*), pRJ16 (*proAtEPF2::BdEPF2-2*), pJSL190 and pRJ20 (*proAtEPF2::TaEPF1*), pRJ19 (*proAtEPF1::TaEPF2*), pJSL198 (*pBAD::MBdEPF2-1-6xHis*), and pJSL199 (*pBAD::MBdEPF2-2-6xHis*). Plasmid pER8 (Zuo et al., 2000) was used for estradiol-inducible constructs, and the Gateway-cloning system (Invitrogen) was used to generate most constructs for the cross-species complementation studies. See Tables S4 and S5 for details on the plasmid constructions and primers used. Stable transgenic Arabidopsis plants were generated using *Agrobacterium*-mediated transformation by the floral dipping method (Clough and Bent, 1998). More than 30 independent transgenic T1 or T2 lines per construct were screened and subjected to detailed phenotypic characterization.

RNA extraction and quantitative RT-PCR analysis

Total RNA from different plant tissues of Brachypodium, wheat, and 10-day-old Arabidopsis transgenic seedlings grown on ½ MS plates with or without 30 μM estradiol were isolated using the RNeasy Plant Mini Kit (Qiagen) and treated with

DNaseI (Qiagen) according to the manufacturer's instructions. The first-strand cDNA was generated by iScript cDNA Synthesis kit (Bio-Rad) using 1.2 µg of RNA except for wheat for which 100 ng of RNA was used, diluted 1:10 in double distilled water, and then used as a template for qPCR analysis. RT-qPCR analysis was performed using a CFX96 real-time PCR detection system (Bio-Rad) using SsoAdvanced Universal SYBR Green Supermix (Bio-Rad) and standard qPCR conditions in at least three technical and three biological replicates. Data was normalized against *eIF4A*, *BdUBC18* (Hong et al., 2008), and *TaRP15* (Shaw et al., 2012) for genes in Arabidopsis, Brachypodium, and wheat, respectively. The Pfaffl method (Pfaffl, 2001) was used to calculate the relative expression levels of the target genes. Gene specific primers used to detect transcripts are listed in Table S5.

Microscopy and quantitative analysis of stomatal phenotype

Confocal images were taken using a Nikon C2 operated by NIS-Elements (Nikon) as described previously (Tamnanloo et al., 2018). All image processing was performed using Fiji software, and the images were false colored using Photoshop CS6 (Adobe). For quantitative analysis, the central area of abaxial cotyledons of 10-day-old Arabidopsis seedlings and the base of the first leaves of 6- to 8-day-old Brachypodium seedlings were stained with toluidine blue O (TBO) (Sigma) as previously reported (Hara et al., 2009), and images were taken using a Nikon Eclipse TiE microscope equipped with a DsRi2 digital camera (Nikon). The number of stomata and other epidermal cells in each photograph were counted and converted into both the density and index measurements for each cell type. The statistically significant differences in a panel of different genotypes was determined by either a Tukey's HSD test after a one-way ANOVA ($P < 0.05$) or a Student's *t*-test with P values of **< 0.001 or *< 0.01.

Chemical treatments

Transgenic Arabidopsis seedlings carrying estradiol-inducible *EPF* and Brachypodium and wheat homolog constructs were germinated on ½ MS medium in the absence or presence of 30 µM estradiol (Sigma) or 1-day-old transgenic

seedlings grown in ½ MS liquid medium were treated with or without 10 μM estradiol. The induction of *EPF* gene expression was confirmed by RT-qPCR analysis. The phenotypic consequence of induction was examined by observing the epidermal phenotype of cotyledons using a confocal microscope.

Production of peptides and bioassays

Expression and purification of Brachypodium MBdEPF2-1 and MBdEPF2-2 peptides were performed as described previously (Lee et al., 2012). These two recombinant peptides and chemically synthesized Brachypodium MBdSTOMAGEN-1 and MBd2g53661 (Invitrogen) were dissolved in 20 mM Tris-HCl, pH 8.8, and 50 mM NaCl and refolded (Mini dialysis kit, MWCO:1,000, GE Healthcare) for 3 d at 4 °C using glutathione (reduced and oxidized forms; Sigma) and L-arginine ethyl ester dihydrochloride (Sigma). The peptides were further dialysed twice against 50 mM Tris-HCl, pH 8.0 for 1.5 d to remove glutathione. For bioassays, either a buffer solution alone (mock: 50 mM Tris-HCl at pH 8.0) or Brachypodium EPF peptides (2.5 μM) in buffer solution were applied to 1-day-old Col and Bd21-3 seedlings in ½ MS liquid medium. After 6-8 days of further incubation, the epidermal phenotypes of abaxial Arabidopsis cotyledons and Brachypodium leaves were examined with a Nikon C2 confocal microscope and/or a Nikon Eclipse TiE microscope after TBO staining.

Acknowledgements

We thank Dr. Keiko Torii for sharing seeds and plasmids with us, and we thank Sahar Soodbakhsh for plant care.

Competing interests

The authors declare no competing or financial interests.

Funding

This work was supported by funding from the Natural Sciences and Engineering Research Council (NSERC) Discovery program of Canada to J.S.L. and Alberta Innovates Bio Solutions and Alberta Wheat Commission to J.S.L. and N.A.F. X.W. was supported by the China Scholarship Council and J.S.L. was a Concordia University Research Chair.

References

Alaux, M., Rogers, J., Letellier, T., Flores, R., Alfama, F., Pommier, C., Mohellibi, N., Durand, S., Kimmel, E., Michotey, C., et al. (2018). Linking the International Wheat Genome Sequencing Consortium bread wheat reference genome sequence to wheat genetic and phenomic data. *Genome Biol* **19**, 111.

Cai, S., Papanatsiou, M., Blatt, M. R. and Chen, Z. H. (2017). Speedy Grass Stomata: Emerging Molecular and Evolutionary Features. *Mol Plant* **10**, 912-914.

Caine, R. S., Yin, X., Sloan, J., Harrison, E. L., Mohammed, U., Fulton, T., Biswal, A. K., Dionora, J., Chater, C. C., Coe, R. A., et al. (2019). Rice with reduced stomatal density conserves water and has improved drought tolerance under future climate conditions. *New Phytol* **221**, 371-384.

Chen, Z. H., Chen, G., Dai, F., Wang, Y., Hills, A., Ruan, Y. L., Zhang, G., Franks, P. J., Nevo, E. and Blatt, M. R. (2017). Molecular Evolution of Grass Stomata. *Trends Plant Sci* **22**, 124-139.

Clough, S. J. and Bent, A. F. (1998). Floral dip: a simplified method for Agrobacterium-mediated transformation of Arabidopsis thaliana. *Plant J* **16**, 735-743.

Dunn, J., Hunt, L., Afsharinafar, M., Meselmani, M. A., Mitchell, A., Howells, R., Wallington, E., Fleming, A. J. and Gray, J. E. (2019). Reduced stomatal density in bread wheat leads to increased water-use efficiency. *J Exp Bot* **70**, 4737-4748.

Hara, K., Kajita, R., Torii, K. U., Bergmann, D. C. and Kakimoto, T. (2007). The secretory peptide gene EPF1 enforces the stomatal one-cell-spacing rule. *Genes Dev* **21**, 1720-1725.

Hara, K., Yokoo, T., Kajita, R., Onishi, T., Yahata, S., Peterson, K. M., Torii, K. U. and Kakimoto, T. (2009). Epidermal cell density is autoregulated via a secretory peptide, EPIDERMAL PATTERNING FACTOR 2 in Arabidopsis leaves. *Plant Cell Physiol* **50**, 1019-1031.

Hepworth, C., Caine, R. S., Harrison, E. L., Sloan, J. and Gray, J. E. (2018). Stomatal development: focusing on the grasses. *Curr Opin Plant Biol* **41**, 1-7.

Hetherington, A. M. and Woodward, F. I. (2003). The role of stomata in sensing and driving environmental change. *Nature* **424**, 901-908.

Hong, S. Y., Seo, P. J., Yang, M. S., Xiang, F. and Park, C. M. (2008). Exploring valid reference genes for gene expression studies in Brachypodium distachyon by real-time PCR. *BMC Plant Biol* **8**, 112.

Huang, X. and Madan, A. (1999). CAP3: A DNA sequence assembly program. *Genome Res* **9**, 868-877.

Hughes, J., Hepworth, C., Dutton, C., Dunn, J. A., Hunt, L., Stephens, J., Waugh, R., Cameron, D. D. and Gray, J. E. (2017). Reducing Stomatal Density in Barley Improves Drought Tolerance without Impacting on Yield. *Plant Physiol* **174**, 776-787.

Hunt, L., Bailey, K. J. and Gray, J. E. (2010). The signalling peptide EPFL9 is a positive regulator of stomatal development. *New Phytol* **186**, 609-614.

Hunt, L. and Gray, J. E. (2009). The signaling peptide EPF2 controls asymmetric cell divisions during stomatal development. *Curr Biol* **19**, 864-869.

International Wheat Genome Sequencing, C. (2014). A chromosome-based draft sequence of the hexaploid bread wheat (Triticum aestivum) genome. *Science* **345**, 1251788.

International Wheat Genome Sequencing, C., investigators, I. R. p., Appels, R., Eversole, K., Feuillet, C., Keller, B., Rogers, J., Stein, N., investigators, I. w.-g. a. p., Pozniak, C. J., et al. (2018). Shifting the limits in wheat research and breeding using a fully annotated reference genome. *Science* **361**.

Kondo, T., Kajita, R., Miyazaki, A., Hokoyama, M., Nakamura-Miura, T., Mizuno, S., Masuda, Y., Irie, K., Tanaka, Y., Takada, S., et al. (2010). Stomatal density is controlled by a mesophyll-derived signaling molecule. *Plant Cell Physiol* **51**, 1-8.

Kosentka, P. Z., Overholt, A., Maradiaga, R., Mitoubsi, O. and Shpak, E. D. (2019). EPFL Signals in the Boundary Region of the SAM Restrict Its Size and Promote Leaf Initiation. *Plant Physiol* **179**, 265-279.

Kumar, S., Stecher, G. and Tamura, K. (2016). MEGA7: Molecular Evolutionary Genetics Analysis Version 7.0 for Bigger Datasets. *Mol Biol Evol* **33**, 1870-1874.

Lawson, T. and Blatt, M. R. (2014). Stomatal size, speed, and responsiveness impact on photosynthesis and water use efficiency. *Plant Physiol* **164**, 1556-1570.

Lee, J. S., Hnilova, M., Maes, M., Lin, Y. C., Putarjunan, A., Han, S. K., Avila, J. and Torii, K. U. (2015). Competitive binding of antagonistic peptides fine-tunes stomatal patterning. *Nature* **522**, 439-443.

Lee, J. S., Kuroha, T., Hnilova, M., Khatayevich, D., Kanaoka, M. M., McAbee, J. M., Sarikaya, M., Tamerler, C. and Torii, K. U. (2012). Direct interaction of ligand-receptor pairs specifying stomatal patterning. *Genes Dev* **26**, 126-136.

Liu, T., Ohashi-Ito, K. and Bergmann, D. C. (2009). Orthologs of Arabidopsis thaliana stomatal bHLH genes and regulation of stomatal development in grasses. *Development* **136**, 2265-2276.

Lu, J., He, J., Zhou, X., Zhong, J., Li, J. and Liang, Y. K. (2019). Homologous genes of epidermal patterning factor regulate stomatal development in rice. *J Plant Physiol* **234-235**, 18-27.

Pfaffl, M. W. (2001). A new mathematical model for relative quantification in real-time RT-PCR. *Nucleic Acids Res* **29**, e45.

Raissig, M. T., Abrash, E., Bettadapur, A., Vogel, J. P. and Bergmann, D. C. (2016). Grasses use an alternatively wired bHLH transcription factor network to establish stomatal identity. *Proc Natl Acad Sci U S A* **113**, 8326-8331.

Raissig, M. T., Matos, J. L., Anleu Gil, M. X., Kornfeld, A., Bettadapur, A., Abrash, E., Allison, H. R., Badgley, G., Vogel, J. P., Berry, J. A., et al. (2017). Mobile MUTE specifies subsidiary cells to build physiologically improved grass stomata. *Science* **355**, 1215-1218.

Shaw, L. M., Turner, A. S. and Laurie, D. A. (2012). The impact of photoperiod insensitive Ppd-1a mutations on the photoperiod pathway across the three genomes of hexaploid wheat (Triticum aestivum). *Plant J* **71**, 71-84.

Sugano, S. S., Shimada, T., Imai, Y., Okawa, K., Tamai, A., Mori, M. and Hara-Nishimura, I. (2010). Stomagen positively regulates stomatal density in Arabidopsis. *Nature* **463**, 241-244.

Takata, N., Yokota, K., Ohki, S., Mori, M., Taniguchi, T. and Kurita, M. (2013). Evolutionary relationship and structural characterization of the EPF/EPFL gene family. *PLoS One* **8**, e65183.

Tameshige, T., Okamoto, S., Lee, J. S., Aida, M., Tasaka, M., Torii, K. U. and Uchida, N. (2016). A Secreted Peptide and Its Receptors Shape the Auxin Response Pattern and Leaf Margin Morphogenesis. *Curr Biol* **26**, 2478-2485.

Tamnanloo, F., Damen, H., Jangra, R. and Lee, J. S. (2018). MAP KINASE PHOSPHATASE1 Controls Cell Fate Transition during Stomatal Development. *Plant Physiol* **178**, 247-257.

Uchida, N., Lee, J. S., Horst, R. J., Lai, H. H., Kajita, R., Kakimoto, T., Tasaka, M. and Torii, K. U. (2012). Regulation of inflorescence architecture by intertissue layer ligand-receptor communication between endodermis and phloem. *Proc Natl Acad Sci U S A* **109**, 6337-6342.

Uchida, N. and Tasaka, M. (2013). Regulation of plant vascular stem cells by endodermis-derived EPFL-family peptide hormones and phloem-expressed ERECTA-family receptor kinases. *J Exp Bot* **64**, 5335-5343.

Wang, H., Guo, S., Qiao, X., Guo, J., Li, Z., Zhou, Y., Bai, S., Gao, Z., Wang, D., Wang, P., et al. (2019). BZU2/ZmMUTE controls symmetrical division of guard mother cell and specifies neighbor cell fate in maize. *PLoS Genet* **15**, e1008377.

Wu, Z., Chen, L., Yu, Q., Zhou, W., Gou, X., Li, J. and Hou, S. (2019). Multiple transcriptional factors control stomata development in rice. *New Phytol* **223**, 220-232.

Yin, X., Biswal, A. K., Dionora, J., Perdigon, K. M., Balahadia, C. P., Mazumdar, S., Chater, C., Lin, H. C., Coe, R. A., Kretzschmar, T., et al. (2017). CRISPR-Cas9 and CRISPR-Cpf1 mediated targeting of a stomatal developmental gene EPFL9 in rice. *Plant Cell Rep* **36**, 745-757.

Zuo, J., Niu, Q. W. and Chua, N. H. (2000). Technical advance: An estrogen receptor-based transactivator XVE mediates highly inducible gene expression in transgenic plants. *Plant J* **24**, 265-273.

Figures

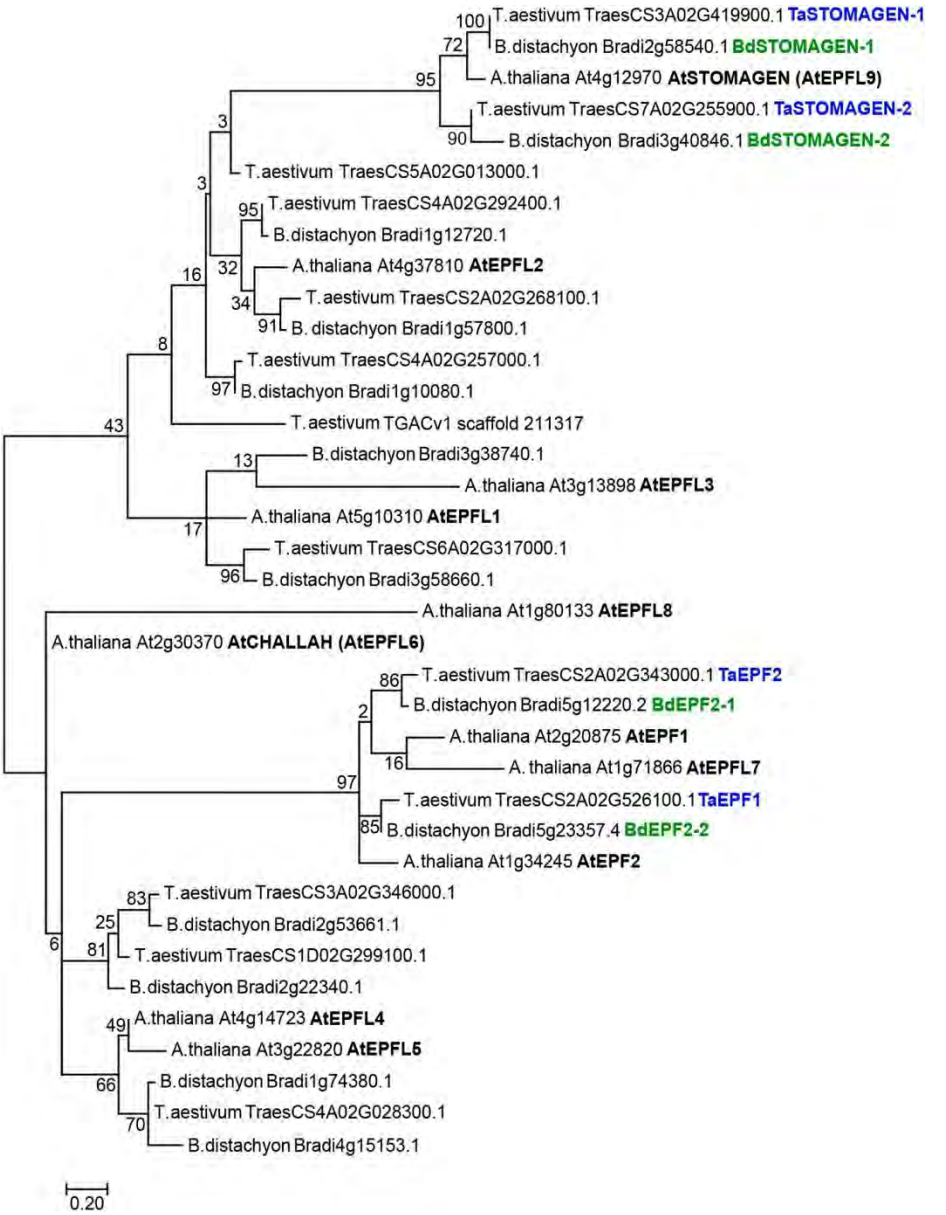

Fig. 1. Identification of grass EPF family peptides.

Phylogenetic tree of the EPF family members in Arabidopsis, Brachypodium, and wheat. The tree is constructed in MEGA7 (Kumar et al., 2016) using the amino acid sequences of the predicted mature C-terminal region of the EPF family members (MEPFs) and their homologs. The tree is drawn to scale, with branch lengths measured in the number of substitutions per site. MEPF sequence alignment is shown in Fig. S1B.

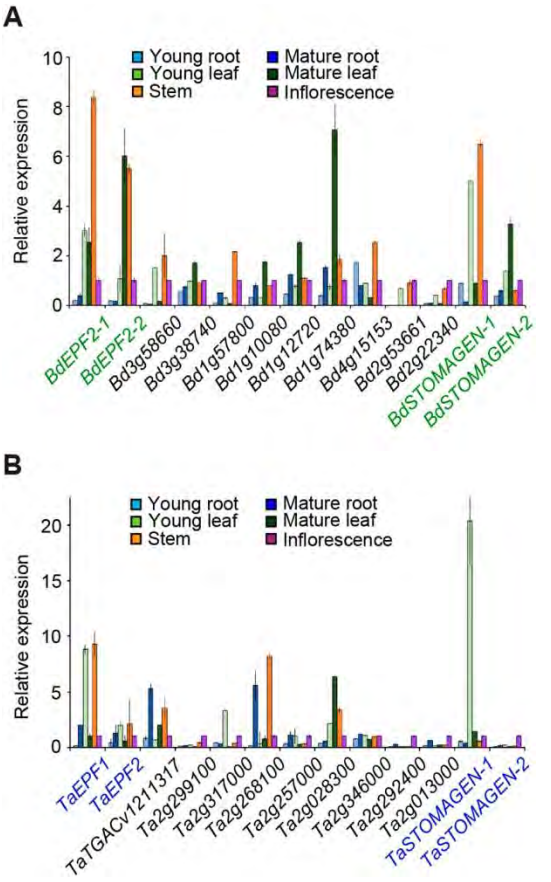

Fig. 2. Expression pattern of *EPF* family members in Brachypodium and wheat. (A) Relative expression levels of EPF homologs in different Brachypodium tissues: young roots, mature roots, young leaves, mature leaves, stems and inflorescences. Young roots and leaves were obtained from 5–7 days-post-germination (dpg) seedlings. Samples of mature roots, leaves and stems at 10 weeks post-germination and inflorescences at 10 days after flowering were used. *BdUBC18* was used as an internal control and the data for inflorescences were set to 1. Error bars = means with SE (n = 3). (B) Relative expression levels of EPF homologs in different wheat tissues: young roots, mature roots, young leaves, mature leaves, stems, and inflorescences. Young roots and leaves were obtained from 3–5 dpg seedlings. Mature roots, leaves, and stems at 10 weeks post-germination and inflorescences at 10 days after flowering were used. *TaRP15* was used as an internal control and the data for inflorescences were set to 1. Error bars = means with SE (n = 3).

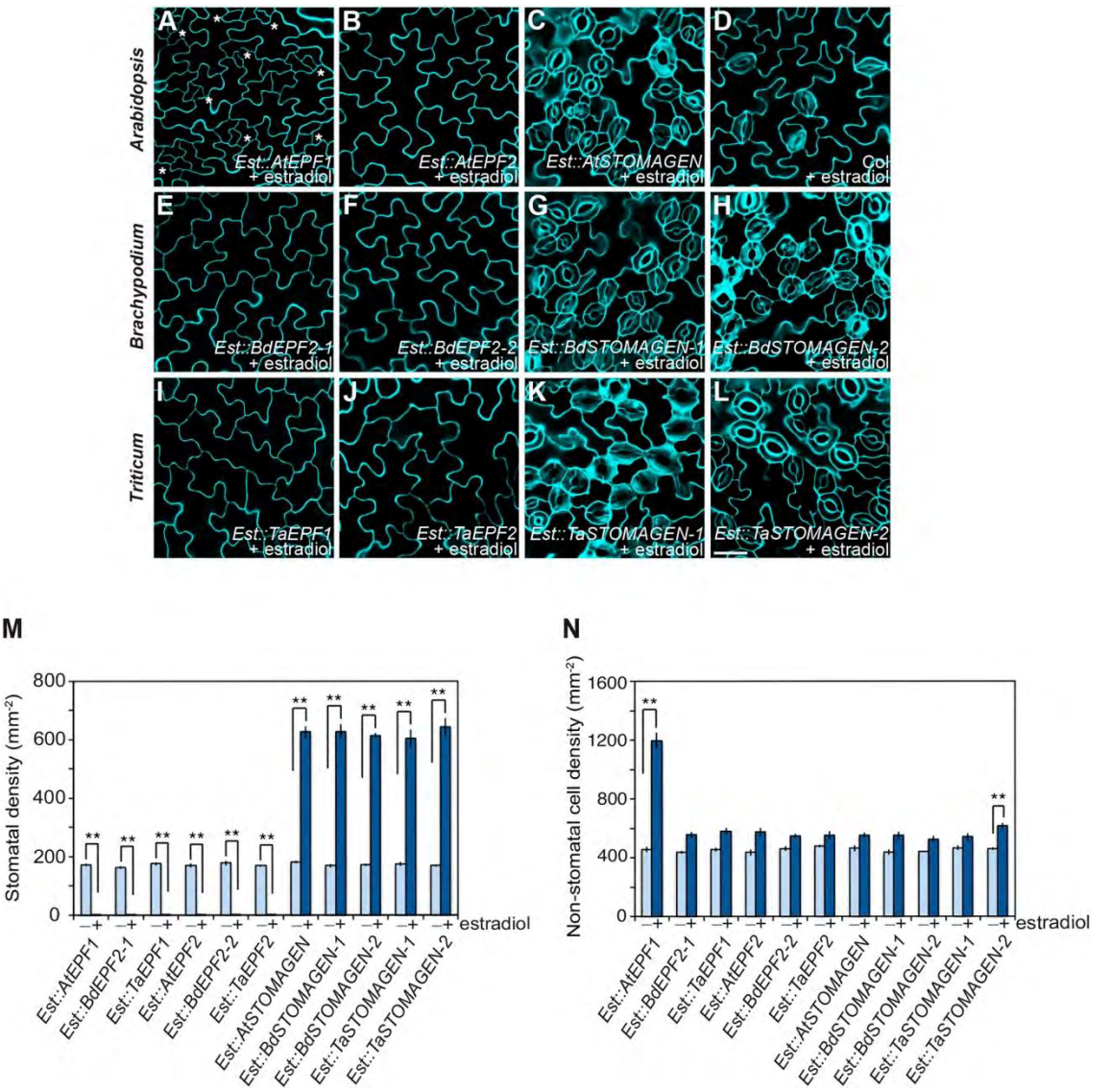

Fig. 3. Ectopic expression of grass stomatal EPF homologs exhibit stomatal development defects in Arabidopsis.

(A-L) Representative confocal images of the abaxial cotyledon epidermis of 10-day-old Arabidopsis transgenic seedlings carrying oestradiol-induced constructs of well-known stomatal EPF family peptides in Arabidopsis; (A) *Est::AtEPF1,* (B) *Est::AtEPF2,* (C) *Est::AtSTOMAGEN,* and the stomatal EPF homologs in Brachypodium; (E) *Est::BdEPF2-1,* (F) *Est::BdEPF2-2,* (G) *Est::BdSTOMAGEN-1,* (H) *Est::BdSTOMAGEN-2* and the wheat stomatal EPF homologs; (I) *Est::TaEPF1* (J), *Est::TaEPF2,* (K) *Est::TaSTOMAGEN-1* and (L) *Est::TaSTOMAGEN-2* . Arabidopsis

Columbia (Col) wild-type seedlings in the presence of estradiol (D) and uninduced controls show no effects on stomatal development (see Fig. S2 and Fig. S3). Asterisks in (A) indicate arrested stomatal precursors. Cells were outlined by propidium iodide staining (cyan), and images were taken under the same magnification. Scale bar = 30 μm. (M, N) Quantitative analysis of 10-day-old abaxial cotyledon epidermis. (M) Stomatal density (number of stomata per mm^2) and (N) non-stomatal epidermal cell density (number of non-stomatal cells per mm^2) from Arabidopsis transgenic seedlings harboring constructs of each of the oestradiol-inducible stomatal EPF peptides in Arabidopsis, and their grass homologs in Brachypodium and wheat. – = no induction and + = induced by oestradiol. Overexpression of *AtEPF1/AtEPF2*-like genes from wheat and Brachypodium led to an epidermis devoid of all stomatal lineage cells, a phenotype identical to induced Arabidopsis *EPF2,* but not like the *EPF1* overexpression. In contrast, induced *STOMAGEN*-like genes in grass increased stomatal density and clustering, a phenotype identical to the Arabidopsis *STOMAGEN* overexpressor. Significant difference compared to the uninduced transgenic seedlings: $^{**}P < 0.0001$ by Student's *t* test. n = 8–9 for each genotype. The experiments were repeated three times with similar results. Bars = means. Error bars are the s.e.m. For a complete set of phenotypes and expression data of multiple independent transgenic plants, see Fig. S2 and Fig. S3.

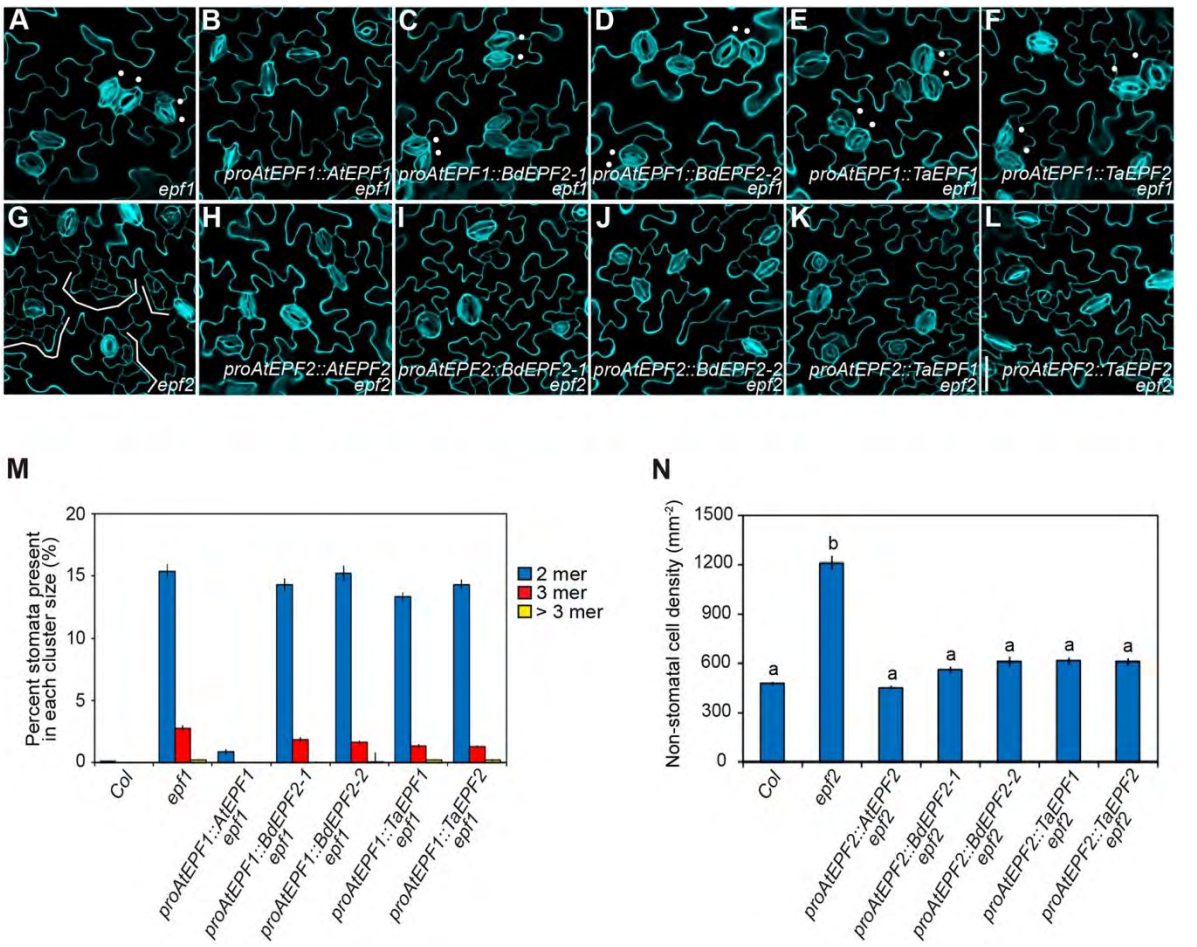

Fig. 4. Complementation of *Arabidopsis epf2* mutants by grass *EPF1/EPF2* homologs.

(A-F) Confocal images of 10-day-old abaxial cotyledons of the (A) Arabidopsis *epf1* mutant (B) *epf1* expressing *proAtEPF1::AtEPF1* , (C) *proAtEPF1::BdEPF2-1* , (D) *proAtEPF1::BdEPF2-2*, (E) *proAtEPF1::TaEPF1*, and (F) *proAtEPF1::TaEPF2*. Expression of *AtEPF1*, but not any of the grass *EPF1/EPF2*-like genes, driven by the Arabidopsis *EPF1* promoter rescues the stomatal pairing phenotype (dots) of Arabidopsis *epf1* mutant. (G-L) Confocal images of 10-day-old abaxial cotyledons of (G) the Arabidopsis *epf2* mutant, (H) *epf2* expressing *proAtEPF2::AtEPF2*, (I) *proAtEPF2::BdEPF2-1*, (J) *proAtEPF2::BdEPF2-2*, (K) *proAtEPF2::TaEPF1,* and (L) *proAtEPF2::TaEPF2*. Excessive entry divisions (brackets), which is the typical phenotype of the Arabidopsis *epf2* mutant, were complemented by *AtEPF2* as well as grass *EPF1/EPF2*-like genes, which were expressed under the control of the

Arabidopsis EPF2 promoter. All confocal images were taken under the same magnification. Scale bars = 30 μm. (M) Percentage of stomata present in each cluster size (in %) in the *epf1* mutant and the *epf1* mutant expressing *AtEPF1* and *EPF1/EPF2*-like genes in Brachypodium and wheat. (N) Non-stomatal epidermal cell density of 10-day-old abaxial cotyledons of the *epf2* mutant and the *epf2* mutant expressing *AtEPF2* and grass *EPF1/EPF2* homologs. Genotypes without significantly different phenotypes were grouped together with the same letter ($P < 0.05$, Tukey's HSD test after a one-way ANOVA). n = 15–17 for each genotype. Bars = means. Error bars = SE. See also Fig. S5 and Fig. S6.

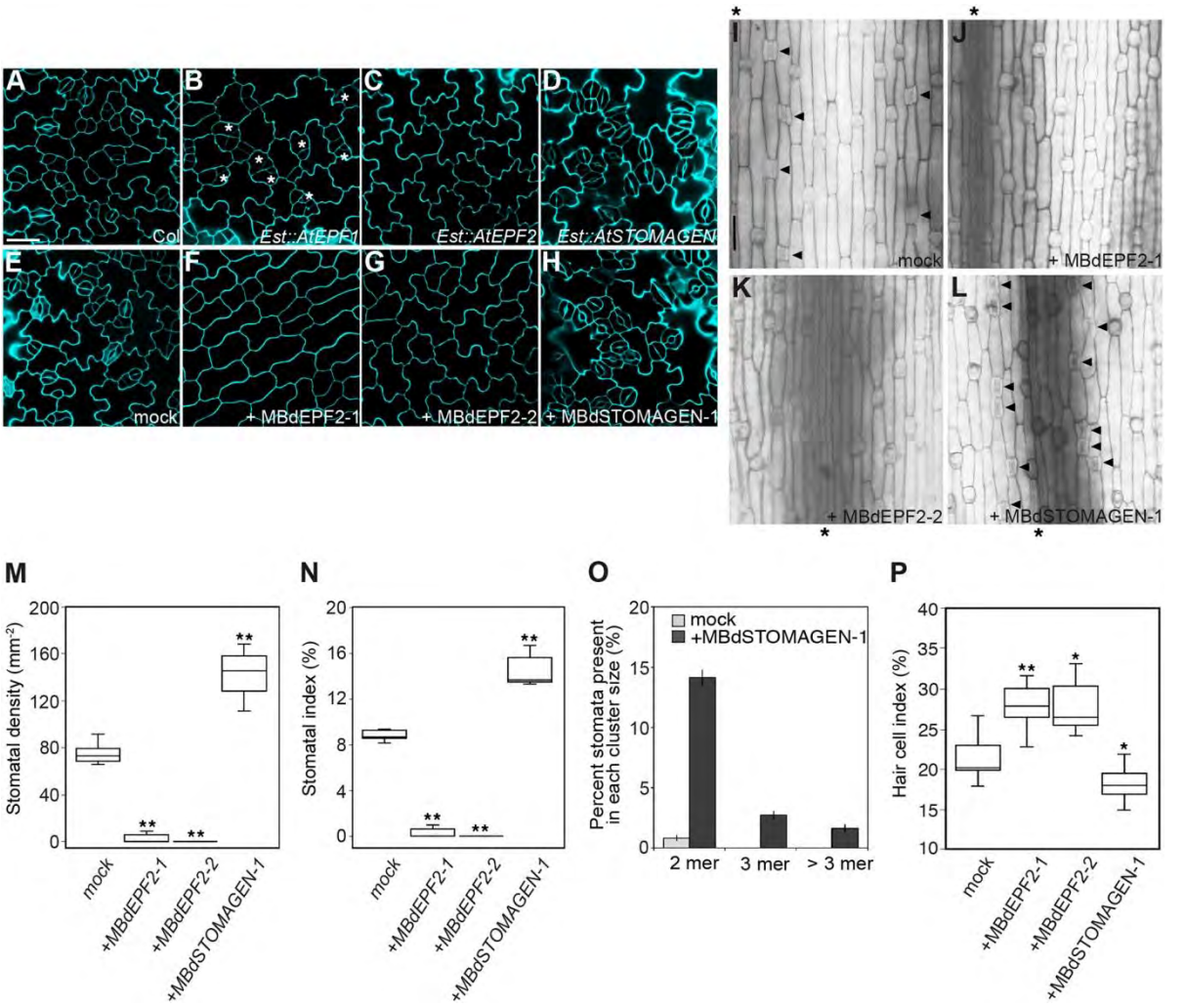

Fig. 5. Effects of the application of bioactive Brachypodium EPF peptides on epidermal development.

(A-D) Representative confocal images of abaxial cotyledons of (A) *Arabidopsis* wild-type (Col), and (B) transgenic seedlings carrying oestradiol-inducible constructs of Arabidopsis EPF peptides, *Est::AtEPF1*, (C) *Est::AtEPF2*, and (D) *Est::AtSTOMAGEN* grown in 1/2 MS liquid medium with estradiol. The asterisks in (B) indicate arrested stomatal precursor cells. (E-H) Abaxial epidermis of cotyledons of (E) Col seedlings grown in a buffer solution (mock), (F) 2 µM MBdEPF2-1, (G) 2 µM MBdEPF2-2, or (H) 2 µM MBdSTOMAGEN-1. Both bioactive, recombinant EPF1/EPF2-like peptides from Brachypodium, MBdEPF2-1 and MBdEPF2-2, inhibit stomatal lineage initiation, while synthetic MBdSTOMAGEN-1 peptide promotes

stomatal clustering and density in Arabidopsis. Images were taken under the same magnification. Scale bar = 30 μm. (I-L) Optical microscopy images of abaxial epidermis of the first leaves of (I) Brachypodium wild-type (Bd21-3) seedlings grown in 1/2 MS liquid medium with a buffer solution (mock), (J) 2 μM MBdEPF2-1, (K) 2 μM MBdEPF2-2, or (L) 2 μM MBdSTOMAGEN-1. Arrowheads indicate stomata which are always found in specific cell files adjacent to veins (marked by asterisks) in Brachypodium. Images were taken under the same magnification. Scale bar = 50 μm. (M-P) Quantitative analysis of abaxial leaf epidermis of Bd21-3 seedlings without (mock) or with bioactive Brachypodium EPF peptides, MBdEPF2-1, MBdEPF2-2, or MBdSTOMAGEN-1. (M) Stomatal density, (N) stomatal index (% of the number of stomata to the total number of epidermal cells), (O) stomatal cluster distribution (in %), (P) hair cell index (% of the number of hair cells to the total number of epidermal cells). Application of bioactive Brachypodium MBdEPF2-1 or MBdEPF2-2 peptide inhibits stomatal development accompanied by default development as hair cells increased in stomatal cell files in the Brachypodium epidermis. In contrast, MBdSTOMAGEN-1 peptide increases stomatal density and clustering in Brachypodium. Peptide application experiments were performed at least five times with similar results. n = 6–11 for each treatment. Bars = means. Error bars = SE. ** P < 0.001, *P < 0.01 (based on Student's t-test with data from mock-treated Bd21-3 seedlings).

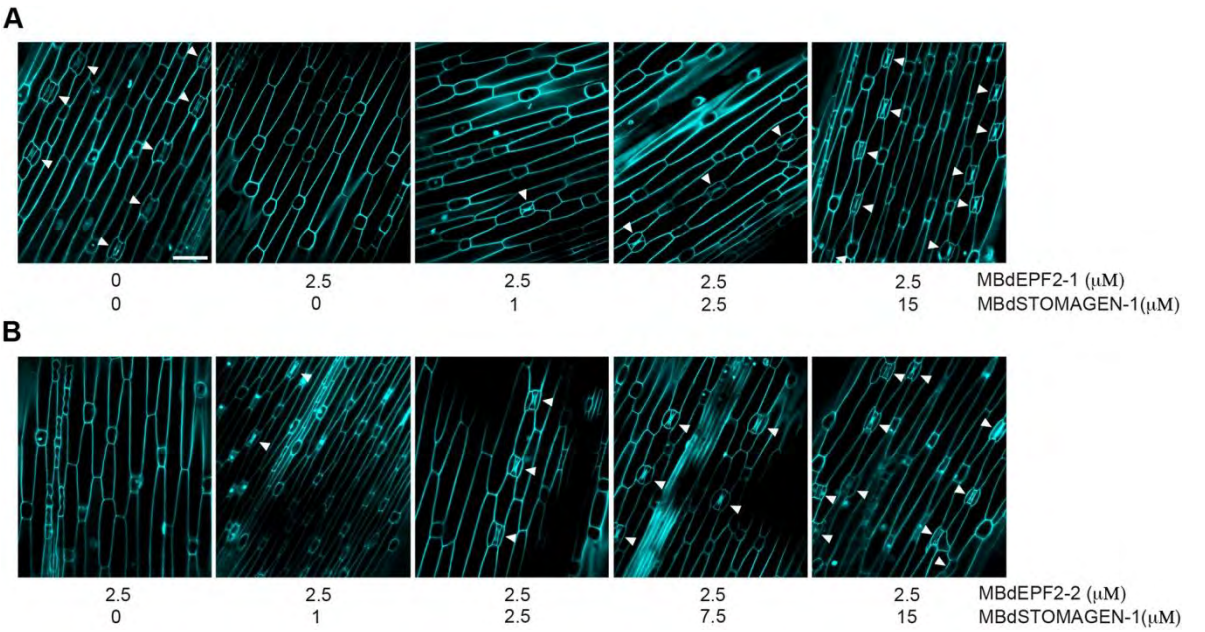

Fig. 6. BdEPF2 activity is antagonized by that of BdSTOMAGEN-1 in Brachypodium.

(A) Brachypodium wild-type (Bd21-3) seedlings treated with a buffer solution, MBdEPF2-1 alone, or mixtures containing MBdEPF2-1 and increasing concentrations of MBdSTOMAGEN-1. (B) Brachypodium Bd21-3 seedlings treated with MBdEPF2-2 alone, or mixtures containing MBdEPF2-2 plus increasing concentrations of MBdSTOMAGEN-1. Biological activity of MBdEPF2 peptides inhibiting grass stomatal development was suppressed by MBdSTOMAGEN-1. Arrowheads indicate stomata which are always found in specific cell files adjacent to veins in Brachypodium leaves. Images were taken under the same magnification. Scale bar = 50 μm. See also Fig. S10 for contrasting results using another EPF-family member in Brachypodium, MBd2g53661 and Fig. S11 for the effect of MBdEPF2-2 in the presence of MBdSTOMAGEN-1.

A

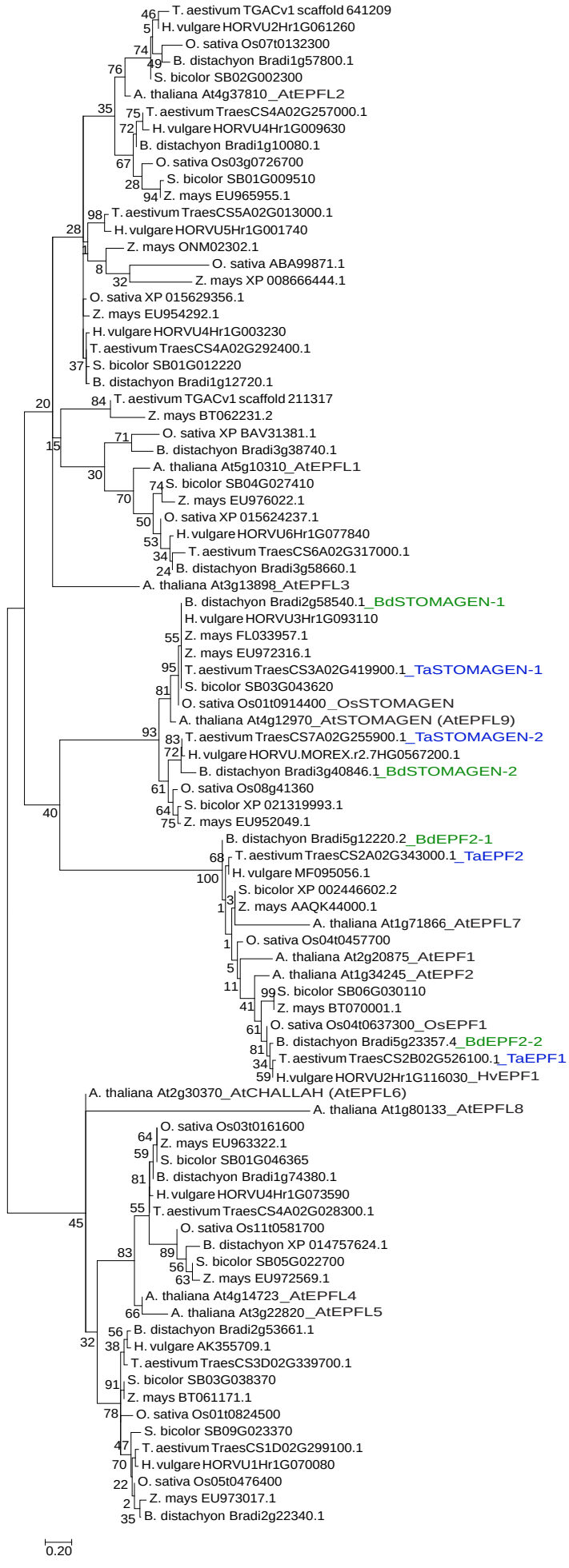

B

```
AtEPF1 (At2g20875)                  (52 aa)  A G S R L P D C S H A C G S C S P C R L V M V S F V C A S V E E A E T C P M A - - - - - - - - - - Y K C M C N N K S Y P V P - - - - - - - - -
AtEPF2 (At1g34245)                  (68 aa)  T G S S L P D C S Y A C G A C S P C K R V M I S F E C S V - - - A E S C S V I - - - - - - - - - - Y R C T C R G R Y Y H V P S R A - - - - - -
BdEPF2-1 (Bd5g12220)                (83 aa)  T G S R L P D C E H A C G P C A P C K R V M V S F R C A L A - - S E S C P V A - - - - - - - - - - Y R C M C R G R F F   V P T L S S A A L P P
BdEPF2-2 (Bd5g23357 )               (139 aa) T G S S L P D C S H A C G P C K P C N R V M V S F K C S I - - - A E P C P M V - - - - - - - - - - Y R C M C K G K C Y P V P S S - - - - - - -
TaEPF1 (Ta2g526100)                 (79 aa)  T G S S L P D C T H A C G A C K P C N R V M I S F K C S I - - - A E P C P M V - - - - - - - - - - Y R C M C K G K C Y P V P S S - - - - - - -
TaEPF2 (Ta2g343000)                 (88 aa)  T G S R L P D C A H A C G A C A P C K R V M V S F R C A E A - - S E S C P I A - - - - - - - - - - Y R C M C H G R F F R V P A L - - - - - - -
AtSTOMAGEN/AtEPFL9 (At4g12970)      (57 aa)  I G S T A P T C T Y - - N E C R G C R - - - - - Y K C R - - - - A E Q V P V E G N D P I N S A Y H Y R C V C H R - - - - - - - - -- - - - - -
BdSTOMAGEN-1 (Bd2g58540)            (77 aa)  I G S I A P I C T Y - - N E C R G C R - - - - - F K C T - - - - A E Q V P V D A N D P M N S A Y H Y K C V C H - - - - - - - - - - - - - - -
BdSTOMAGEN-2 (Bd3g40846)            (76 aa)  V G S R V P T C S Y - - N E C R R C R - - - - G R R C S - - - - A R G V P V D G S D P M S S A Y H Y R C F C H A - - - - - - - - - - - - - - -
TaSTOMAGEN-1 (Ta2g419900)           (77aa)   I G S I A P I C T Y - - N E C R G C R - - - - - S K C T - - - - A E Q V P V D A N D P M N S A Y H Y K C V C H R - - - - - - - - - - - - - - -
TaSTOMAGEN-2 (Ta2g255900)           (73 aa)  V G S R A P T C T Y - - N E C R G C R - - - - - Y R C S - - - - A R G V P V D A T D P M N S A Y H Y R C F C H V - - - - - - - - - - - - - - -
```

Fig. S1. Phylogenetic relationships between Arabidopsis and grass EPF family members.
(A) Phylogenetic tree of the EPF family members in *Arabidopsis thaliana, Brachypodium distachyon, Oryza sativa* (rice), *Hordeum vulgare* (barley), *Sorghum bicolor* (sorghum), *Zea mays* (maize) and *Triticum aestivum* (wheat). The tree was constructed in MEGA7 (Kumar et al., 2016) using the amino acid sequences of the predicted mature C-terminal region of the EPF family members and their grass homologs. The tree was drawn to scale, with branch lengths measured in the number of substitutions per site. (B) The sequence alignment of the predicted mature peptide regions of the stomatal EPFs in Arabidopsis, AtEPF1, AtEPF2 and AtSTOMAGEN, and their homologs in wheat and the model grass organism, Brachypodium. The conserved cysteine residues are highlighted. See also Fig. 1, Table S1-S3.

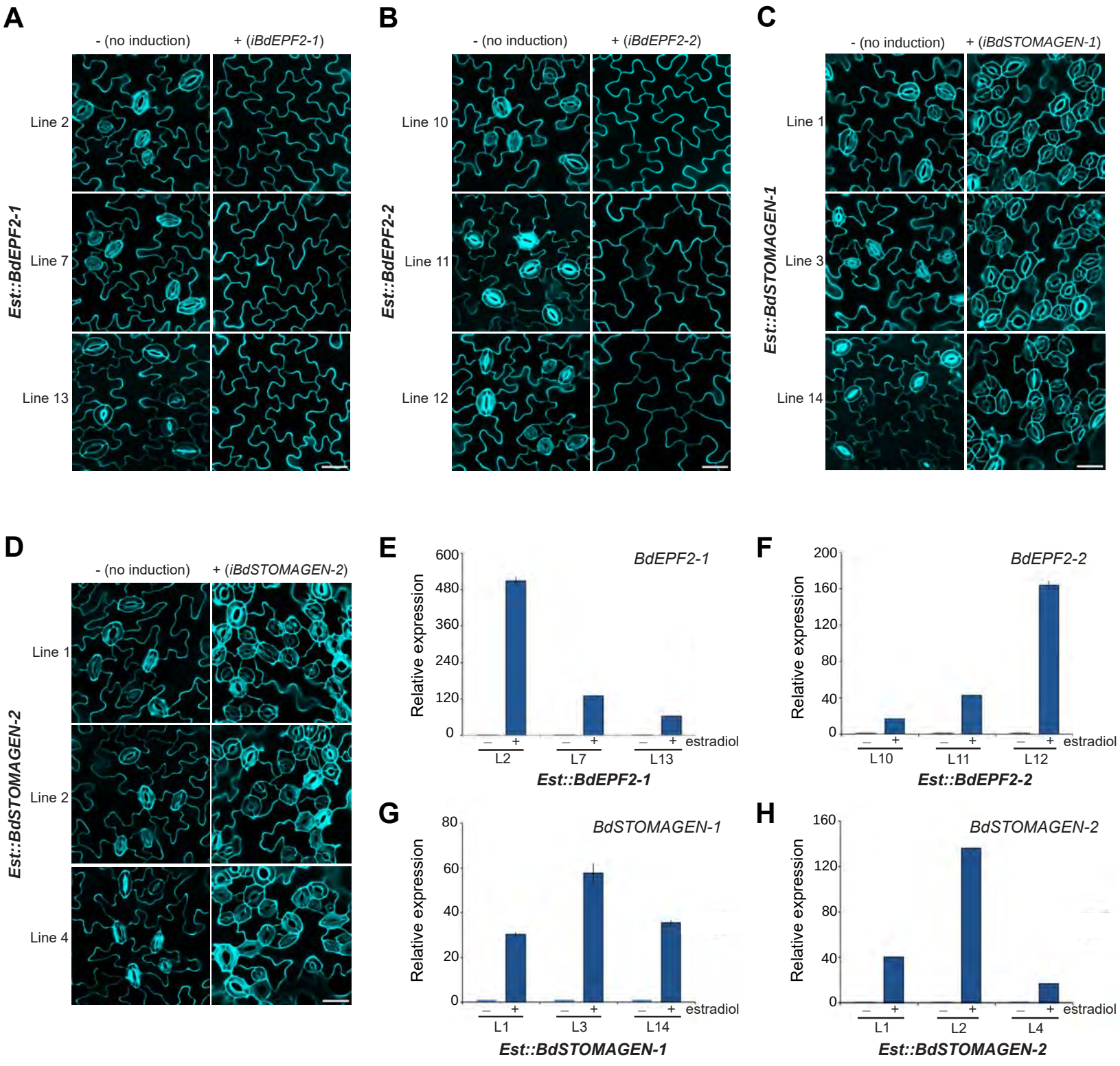

Fig. S2. Epidermis phenotype of induced overexpression of Brachypodium EPF stomatal homologs in multiple independent Arabidopsis transgenic lines.
(A-D) Representative confocal images of abaxial cotyledon epidermis from 10-day-old seedlings of three independent Arabidopsis transgenic lines harboring an oestradiol-inducible overexpression construct for each of the four stomatal EPF homologs from Brachypodium: (A) *iBdEPF2-1*, (B) *iBdEPF2-2,* (C) *iBdSTOMAGEN-1,* and (D) *iBdSTOMAGEN-2*. Left panels, no induction (control); right panels, oestradiol induction; each row shows representative images from individual lines. Cells were outlined by propidium iodide staining (cyan), and images were taken under the same magnification. Scale bar = 30 µm. (E-H) RT-qPCR analysis of (E) *BdEPF2-1*, (F) *BdEPF2-2,* (G) *BdSTOMAGEN-1*, and (H) *BdSTOMAGEN-2* transgenes in three independent Arabidopsis transgenic plants carrying oestradiol-inducible overexpression constructs for each of the four Brachypodium stomatal homologs. *eIF4A* was used as an internal control and the data for each uninduced transgenic line was set to 1. Error bars = means with SE (n = 3). For primer sequences, see Table S5.

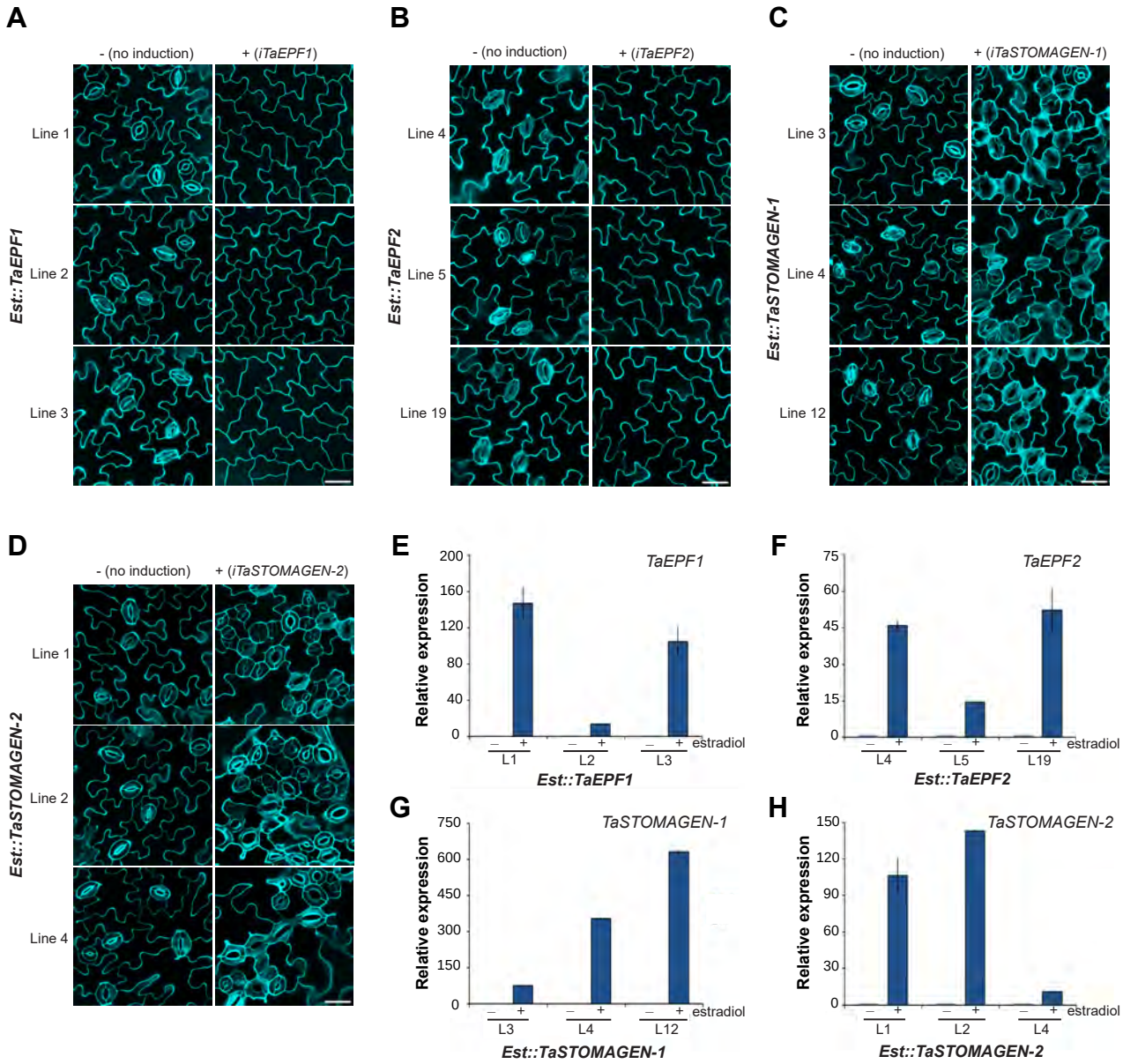

Fig. S3. Epidermis phenotype of induced overexpression of wheat EPF stomatal homologs in multiple independent Arabidopsis transgenic lines.
(A-D) Representative confocal images of abaxial cotyledon epidermis from 10-day-old seedlings of three independent Arabidopsis transgenic lines harboring an oestradiol-inducible overexpression construct for each of four stomatal EPF homologs from wheat: (A) *iTaEPF1*, (B) *iTaEPF2*, (C) *iTaSTOMAGEN-1*, and (D) *iTaSTOMAGEN-2*. Left panels, no induction (control); right panels, oestradiol induction; each row shows representative images from individual lines. Images are taken under the same magnification. Scale bar = 30 µm. (E-H) RT-qPCR analysis of (E) *TaEPF1*, (F) *TaEPF2*, (G) *TaSTOMAGEN-1*, and (H) *TaSTOMAGEN-2* transgenes in three independent Arabidopsis transgenic plants carrying oestradiol-inducible overexpression constructs for each of the four wheat stomatal homologs. *eIF4A* was used as an internal control and the data for each uninduced transgenic line was set to 1. Error bars = means with SE (n = 3). For primer sequences, see Table S5.

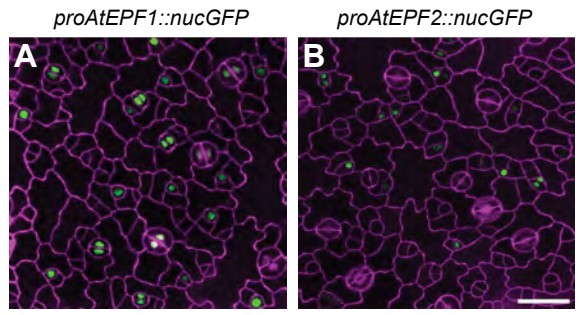

Fig. S4. Expression patterns of stomatal lineage specific *AtEPF1* and *AtEPF2* promoters used in this study.
Representative confocal images of the abaxial developing leaf epidermis of 12-day-old wild-type seedlings carrying the green fluorescent protein (nucGFP)-tagged transcription reporters for the promoters of (A) *AtEPF1* and (B) *AtEPF2*. GFP expression is detected in the nuclei of (A) a subset of later stomatal lineage cells (meristemoids, guard mother cells and young guard cells) and (B) early stomatal lineage cells (meristemoid mother cells and meristemoids) indicating that the two promoter fragments used in this study drive correct expression patterns in the stomatal lineage. Cells were outlined by propidium iodide staining (purple), and images were taken under the same magnification. Scale bar = 30 μm.

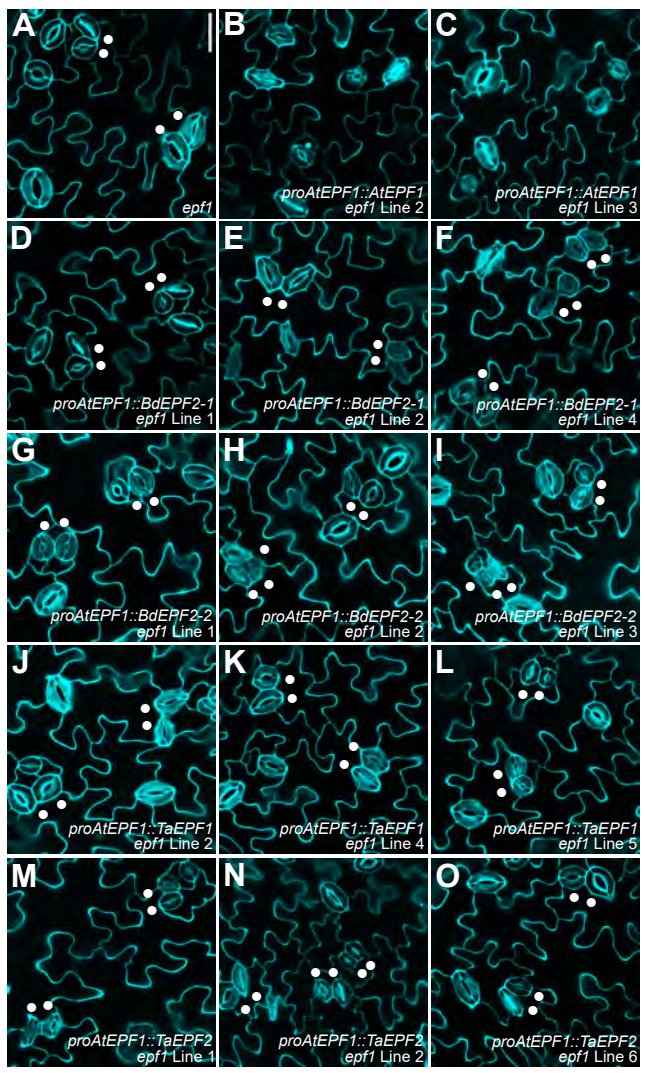

Fig. S5. Complementation of Arabidopsis *epf1* loss-of-function mutants by grass *EPF1/EPF2* homologs.
Shown are representative confocal images of 10-day-old cotyledon epidermis of the (A) Arabidopsis *epf1* mutant, (B,C) two independent transgenic *epf1* plants expressing *proAtEPF1::AtEPF1*, and (D-F) three independent transgenic *epf1* lines expressing *AtEPF1/AtEPF2* homologs from Brachypodium: pro*AtEPF1::BdEPF2-1*, (G-I) *proAtEPF1::BdEPF2-2*, and (J-L) *AtEPF1/AtEPF2* homologs from wheat: *proAtEPF1::TaEPF1*, and (M-O) *proAtEPF1::TaEPF2*. The *epf1* mutation confers stomatal pairing (dots). Unlike the *proAtEPF1::AtEPF1* construct, *AtEPF1/AtEPF2* homologs from Brachypodium and wheat driven by the *AtEPF1* promoter unable to complement the epidermal phenotype of *epf1*. See also Fig. 4A-F,M. All confocal microscopy images were taken under same magnification. Scale bar = 30 µm.

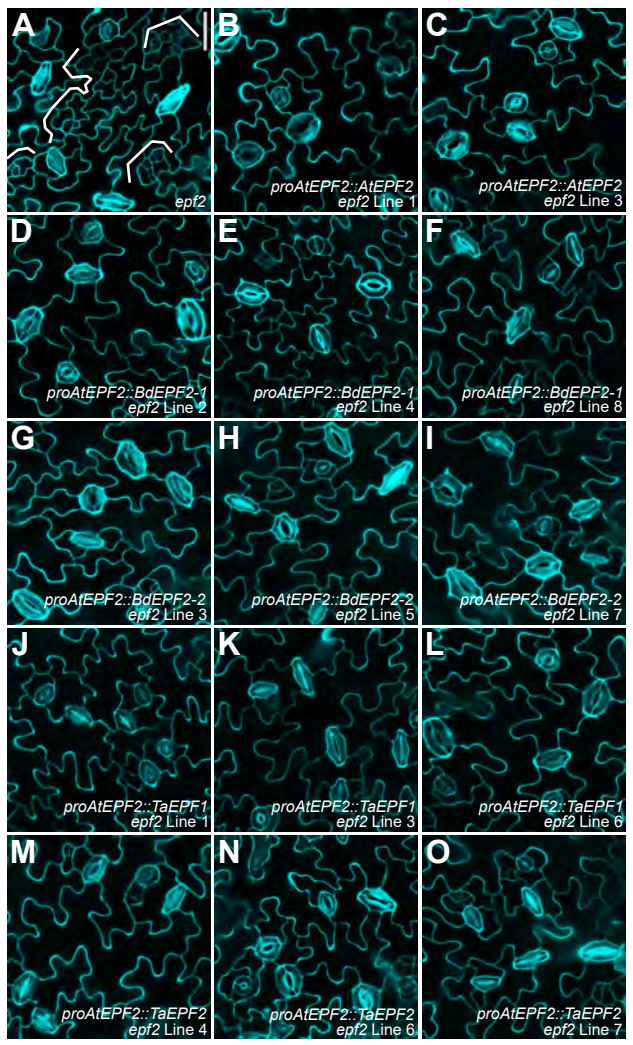

Fig. S6. Complementation of Arabidopsis *epf2* loss-of-function mutants by grass *EPF1/EPF2* homologs.
Representative confocal images of 10-day-old abaxial cotyledons of the (A) Arabidopsis *epf2* mutant, (B,C) two independent transgenic *epf2* plants expressing *proAtEPF2::AtEPF2*, and (D-F) three independent transgenic *epf2* plants expressing *AtEPF1/AtEPF2* homologs from Brachypodium: *proAtEPF2::BdEPF2-1*, (G-I) *proAtEPF2::BdEPF2-2*, and (J-L) *AtEPF1/AtEPF2* homologs from wheat: *proAtEPF2::TaEPF1*, and (M-O) *proAtEPF2::TaEPF2*. The epidermal phenotype of Arabidopsis *epf2* mutants (brackets in A) is rescued by each of the two *AtEPF1/AtEPF2*-like genes from Brachypodium and wheat. See also Fig. 4 G-L,N. All confocal microscopy images were taken under same magnification. Scale bar = 30 μm.

A

MBdEPF2-1, MBdEPF2-2, MBdSTOMAGEN-1, and MBd2g53661 sequence used for bioassays

MBdEPF2-1-mycHis (in pBADg vector)

MKKLLFAIPLVVPFYSHSHSTMELETGSRLPDCEHACGPCAPCKRVMVSFRCALASESCP
VAYRCMCRGRFFRVPTLSSAALPPRIRSFLEQKLISEEDLNSAVDHHHHHH*

MBdEPF2-2-mycHis (in pBADg vector)

MKKLLFAIPLVVPFYSHSHSTMELETGSSLPDCSHACGPCKPCNRVMVSFKCSIAEPCPM
VYRCMCKGKCYPVPSSRIRSFLEQKLISEEDLNSAVDHHHHHH*

MBdSTOMAGEN-1

IGSIAPICTYNECRGCRFKCTAEQVPVDANDPMNSAYHYKCVCHR

MBd2g53661

PGSYPPRCTSKCGSCNPCYPVHVAVPPGVPVTAEYYPEAWRCRCGNRLYMP

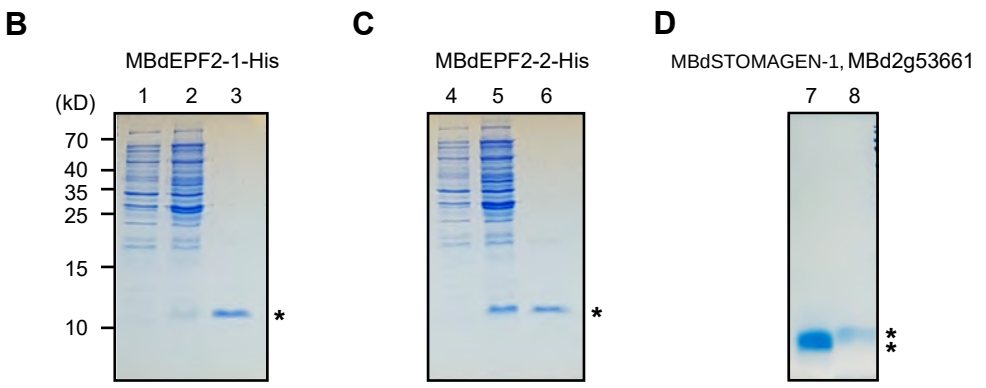

Fig. S7. Amino-acid sequence, expression and purification of bioactive Brachypodium peptides used in this study.
(A) Amino acid sequence of the predicted mature EPF (MEPF) region of MBdEPF2-1, MBdEPF2-2, MBdSTOMAGEN-1, and MBd2g53661 used for bioassays and competition analyses. Underlined: signal sequence from pBADg vector; blue, predicted MBdEPF2-1, MBdEPF2-2, MBdSTOMAGEN-1, and MBd2g53661 sequence; plain, linker, cMyc tag, and His tag. (B-D) Shown are SDS-PAGE gels, stained with Coomassie Brilliant Blue, for expression and purification of bacterially expressed recombinant (B) MBdEPF2-1-His, (C) MBdEPF2-2-His, and (D) synthesized MBdSTOMAGEN-1 and MBd2g53661 after refolding. Lanes 1, 2, 4, and 5: Bacterial lysate carrying MBdEPF2-1 (lanes 1, 2) and MBdEPF2-2 (lanes 4, 5) in the absence (lanes 1, 4) or presence (lanes 2, 5) of L-arabinose for induction; Lanes 3, 6: Purified, dialyzed, and refolded peptide solution of MBdEPF2-1-His (lane 3) and MBdEPF2-2-His (lane 6) and Lanes 7, 8: Refolded synthesized peptide solution of MBdSTOMAGEN-1 (lane 7) and MBd2g53661 (lane 8) used for bioassays and competition analysis in Fig. 5, Fig. 6, Figs. S8-S11. The positions of molecular mass markers in kilodaltons are indicated on the left. Asterisks indicate the size of each His-tagged or synthesized peptide.

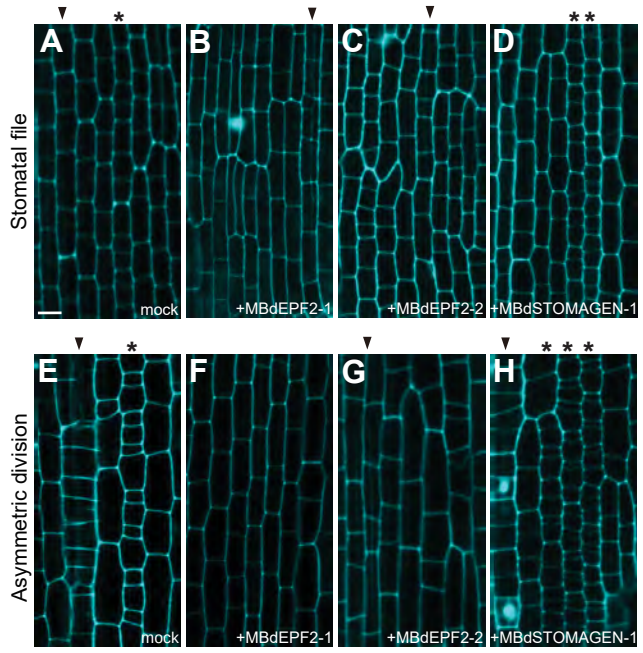

Fig. S8. Early epidermal phenotypes of Brachypodium seedlings treated with bioactive grass EPF peptides. Confocal images of two early developmental stages of grass stomatal development, stomatal file establishment (A-D) and asymmetric division (E-H) stages, in (A,E) Brachypodium wild-type (Bd21-3) seedlings treated with either buffer solution alone (mock) or (B,F) Brachypodium MEPF peptides, MBdEPF2-1, (C,G) MBdEPF2-2, (D,H) and MBdSTOMAGEN-1. The epidermis of Bd21-3 seedlings treated with MBdEPF2-1 or MBdEPF2-2 peptide shows neither smaller cell files nor asymmetric entry divisions in the stomatal rows always flanking to the veins, while application of MBdSTOMAGEN-1 to Bd21-3 seedlings results in ectopic smaller cell files and asymmetric divisions. The asterisks indicate smaller cells (A, D) or asymmetric divisions (E, H) in stomatal lineage rows having stomatal fate. Arrowheads, developing leaf veins. All images are from the base of the developing first Brachypodium leaf at 7-8 days-post-germination (dpg). Scale bar = 10 µm.

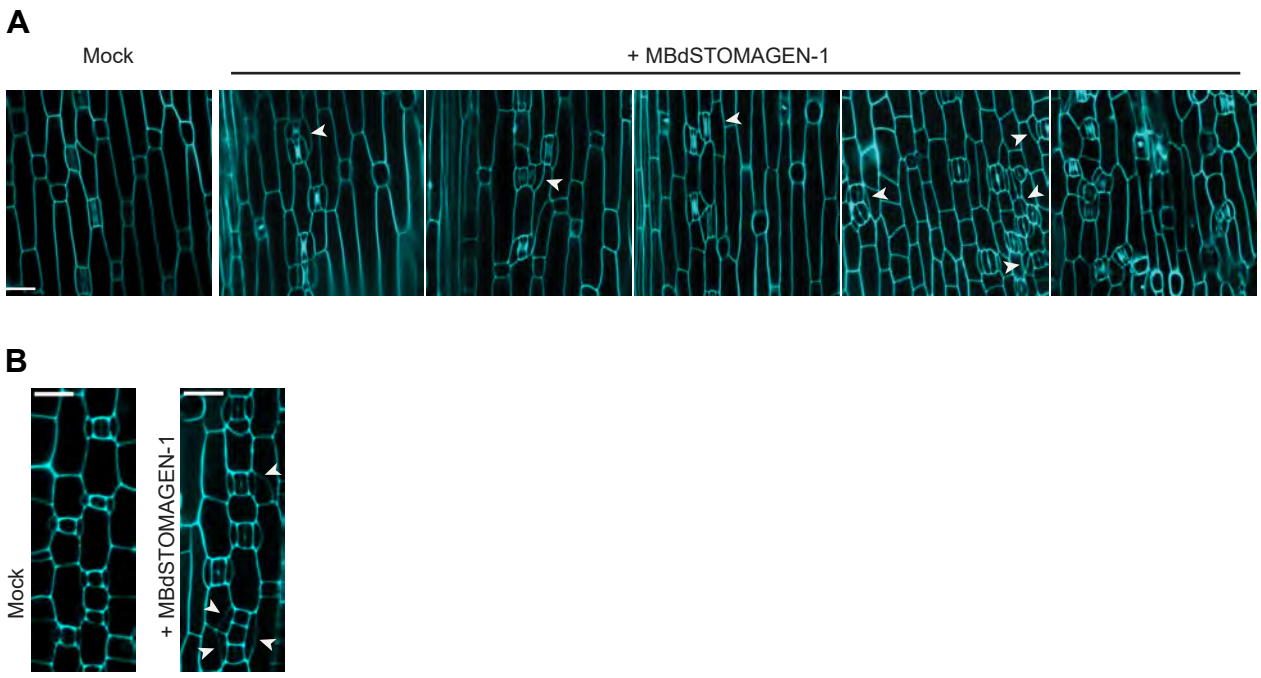

Fig. S9. Bioactive MBdSTOMAGEN-1 peptide, a 45 amino acid cysteine-rich region of the STOMAGEN-like protein in Brachypodium, promotes grass stomatal differentiation and patterning.
(A) Confocal images of the first leaf epidermis illustrating the phenotypic range observed in Brachypodium wild-type (Bd21-3) seedlings treated with 2.5 µM MBdSTOMAGEN-1 peptide. All images are shown at the same scale. Scale bar = 30 µm. (B) Representative confocal images of cells at subsidiary cell formation and guard mother cell division stages of grass stomatal development in Bd21-3 seedlings treated with either buffer only (mock) or 2.5 µM MBdSTOMAGEN-1 peptide. All images are shown at the same scale. Scale bar: 15 µm. Bd21-3 seedlings have 4-celled stomatal complexes composed of two guard cells and two subsidiary cells, and they are separated by at least one non-stomatal cell in particular “stomatal” cell files. Application of refolded MBdSTOMAGEN-1 to Bd21-3 seedlings, however, exhibits stomatal patterning defects. Stomatal clusters sometimes have abnormal subsidiary cell morphologies, additional cell divisions, and are dispersed on the epidermis rather than restricted to the specific cell files typical of grass stomata, indicating the formation of ectopic stomatal rows. The arrowheads indicate examples of abnormal subsidiary cells.

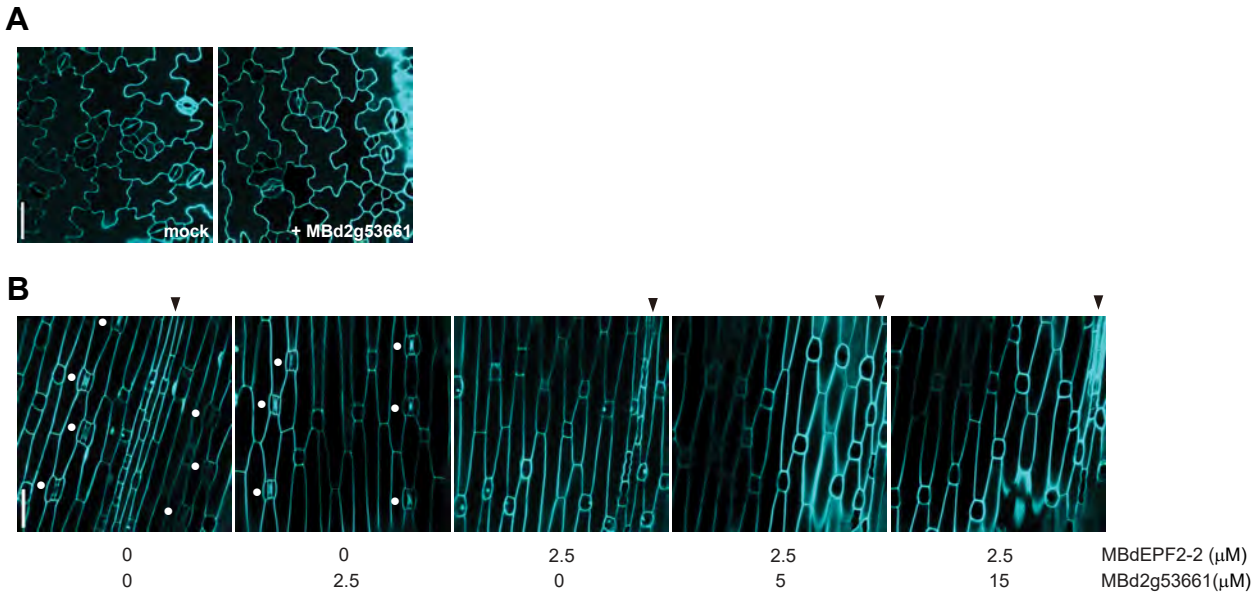

Fig. S10. Unlike BdEPF2 peptides, one of the Brachypodium EPF-family peptides, Bd2g53661, neither controls stomatal development nor competes with BdSTOMAGEN-1.
(A) Confocal images of the cotyledon epidermis of Arabidopsis Col seedlings grown in a buffer solution (mock) or 2.5 μM MBd2g53661. Application of refolded MBd2g53661 peptide does not influence the epidermal development in Arabidopsis. (B) Bd21-3 seedlings treated with a buffer solution, MBd2g53661, MBdEPF2-2, or MBdEPF2-2 co-treated with increasing concentrations of MBdSTOAMGEN-1. MBd2g53661 does not influence the function of MBdEPF2-2 inhibiting grass stomatal development. Dots indicate stomata which are typically found in specific cell files adjacent to veins (marked by arrowheads). Images were taken under the same magnification. Scale bar = 30 μm.

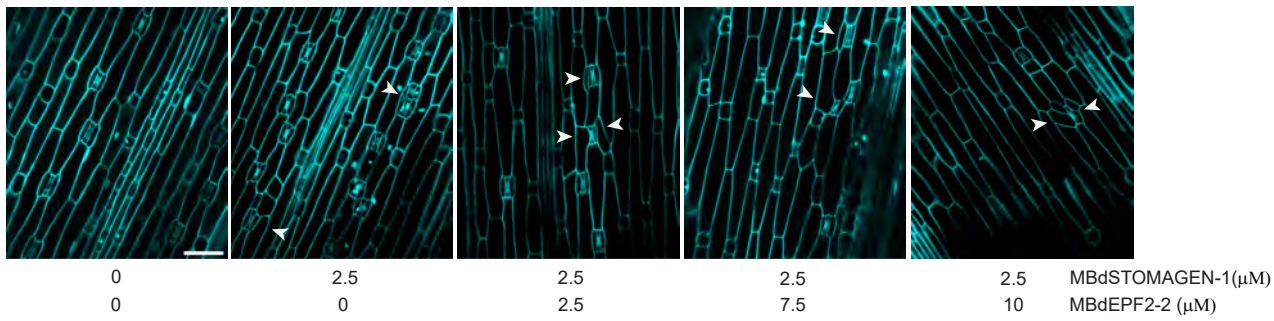

Fig. S11. Biological activity of BdSTOMAGEN-1 in promoting stomatal initiation, but not the subsidiary cell formation, is antagonized by BdEPF2.
Confocal images of Brachypodium Bd21-3 leaf epidermis treated with a buffer solution, MBdSTOMAGEN-1 alone, or mixtures containing MBdSTOAMGEN-1 plus increasing concentrations of MBdEPF2-2 for 7-8 days. Arrowheads indicate stomata with abnormal subsidiary cell morphologies, such as the spanning of two guard cells by a single subsidiary cell or stomata lacking one subsidiary cell. Images were taken under the same magnification. Scale bar = 50 μm.

Table S1

Click here to download Table S1

Table S2

Click here to download Table S2

Table S3

Click here to download Table S3

Table S4

Click here to download Table S4

Table S5

Click here to download Table S5